

## N O T I C E

THIS DOCUMENT HAS BEEN REPRODUCED FROM  
MICROFICHE. ALTHOUGH IT IS RECOGNIZED THAT  
CERTAIN PORTIONS ARE ILLEGIBLE, IT IS BEING RELEASED  
IN THE INTEREST OF MAKING AVAILABLE AS MUCH  
INFORMATION AS POSSIBLE

NASA CR-159782  
PWA-5526-31



THIN FILM TEMPERATURE SENSOR

by

H. P. Grant and J. S. Przybyszewski

(NASA-CR-159782) THIN FILM TEMPERATURE  
SENSOR (Pratt and Whitney Aircraft) 61 p  
HC A04/MF A01 CSCL 14B

N80-17425

Unclas  
G3/35 47246

United Technologies Corporation  
Pratt & Whitney Aircraft  
Commercial Products Division

Prepared for

NATIONAL AERONAUTICS AND SPACE ADMINISTRATION

Lewis Research Center  
Cleveland, Ohio 44135  
Contract NAS3-20768



NASA CR-159782  
PWA-5526-31



THIN FILM TEMPERATURE SENSOR

by

H. P. Grant and J. S. Przybyszewski

United Technologies Corporation  
Pratt & Whitney Aircraft  
Commercial Products Division

Prepared for

NATIONAL AERONAUTICS AND SPACE ADMINISTRATION

Lewis Research Center  
Cleveland, Ohio 44135  
Contract NAS3-20768

## FOREWORD

The work described in this report was accomplished by the Commercial Products Division of Pratt & Whitney Aircraft Group, United Technologies Corporation, under the National Aeronautics and Space Administration Contract NAS3-20768. Mr. Raymond Holanda of the NASA Lewis Research Center was the Project Manager for the program.

This report was prepared by Mr. Howard P. Grant, the Pratt & Whitney Aircraft Program Manager and Mr. John S. Przybylski.

The contributions of Mr. Richard Claing and Mr. Donald Scavone of the Instrument Development Laboratory during the fabrication and testing of the sputtered sensor systems are acknowledged. The assistance and advice of Mr. E. L. Paradis and Dr. J. G. Smeggil of the United Technologies Research Center is also gratefully acknowledged.

PRECEDING PAGE BLANK NOT FILMED

## TABLE OF CONTENTS

Section	Subject	Page
	SUMMARY	1
1.0	INTRODUCTION	2
	1.1 Background	2
	1.2 Objective	4
2.0	TECHNICAL APPROACH	6
3.0	APPARATUS, FABRICATION, AND TEST PROCEDURES	10
	3.1 Preliminary Fabrication and Test Procedures	10
	3.2 Thin Film-to-Lead Wire Connection Fabrication	16
	3.3 Fabrication of Thin Film Thermocouples on Simulated Turbine Blades	21
	3.4 Oven Calibration Equipment and Procedures	23
	3.5 Vibration Test Equipment and Procedures	24
	3.6 High Temperature Exhaust Gas Test Equipment and Procedures	24
4.0	RESULTS AND DISCUSSION	28
	4.1 Preliminary tests	28
	4.2 Thin Film-to-Lead Wire Connection	34
	4.3 Thin Film Thermocouple Systems on Simulated Turbine Blades	35
	4.3.1 Overview	35
	4.3.2 Oven Calibration Tests	35
	4.3.3 Vibration Tests	39
	4.3.4 High Temperature Exhaust Gas Tests	40
5.0	THE PLATINUM FILM ADHERENCE PROBLEM	47
	5.1 Overview	47
	5.2 Principles of Metal Film Adherence	47
	5.3 Approaches to Improving Adherence of Platinum Films on Alumina	49
6.0	CONCLUDING REMARKS	53
7.0	REFERENCES	55

### SUMMARY

The first phase of a three-phase program for the development of thin film surface temperature sensors for application to aircraft engine turbine blades to 1250 K (1800°F) was completed. Candidate sputtered thin film thermocouple systems were fabricated on twenty flat plate specimens of four turbine blade and vane materials and on eight simulated turbine blades. Testing included vibration on three axes, furnace calibrations, and hot hydrocarbon gas flow (low speed oxyacetylene flame) cycling tests to 1250 K. In Phase II the best candidate system will be refined and the environment will be extended to high speed combustor flows on actual turbine blades. In Phase III, the environment will be extended to engine tests on rotating turbine blades.

The systems evolved were platinum vs platinum-10 percent rhodium (Type S) thermocouples of metal films 2  $\mu\text{m}$  thick sputtered directly on an alumina ( $\alpha\text{-Al}_2\text{O}_3$ ) insulating layer 2  $\mu\text{m}$  thick. The alumina layer is produced by deliberate oxidation of an alumina forming NiCoCrAlY or CoCrAlY coating 120  $\mu\text{m}$  thick on the turbine blade or vane material. These coatings were the usual corrosion resistant coatings specified on production engine parts, but applied in this case with special attention to control of surface finish and freedom from contamination. The thin-film-to-lead wire connections were fabricated by a hot compression bonding technique.

Thermal emf was found to be typically 2 percent below ANSI standard Type S thermocouples. The mean time to failure was 42 hours at 1250K (including an average of 15 temperature cycles). Failures were principally due to separation of the platinum film element in the thermocouple system from the alumina surface.

Several techniques to improve the adhesion of platinum were explored. Reactive sputtering, undercoats of chromium and platinum-10 percent rhodium, and field-assisted bonding all showed promise. Further investigation will take place in Phase II.

## 1.0 INTRODUCTION

### 1.1 Background

Turbine blade temperature measurement by blade-mounted sensors is presently accomplished by embedding thermocouples in the blade wall. The uncertainty in this measurement can be as high as 50 K because of the heat path distortion, and uncertainty in exact location of the thermocouple junction. As blade wall thicknesses are decreased due to the inclusion of complex cooling schemes within the blade, the presence of embedded thermocouples becomes more adverse both from a structural and a measurement viewpoint. It would be desirable to have a surface-mounted temperature sensor which did not require removal of any blade material and at the same time was of such minimum mass and thickness that it caused no serious problems with heat path distortion within the blade and gas flow distortion over the blade. A thin film temperature sensor would be compatible with these considerations.

Using various thin film techniques (plating, vacuum evaporation, vacuum sputtering), a sensor can be formed by depositing layers of electrical insulating materials and metals whose thickness is only a few  $\mu$  m. Successful surface thermocouples were obtained in this way by Burger in 1930 (Reference 1), Harris in 1934 (Reference 2), and Benderskey in 1953 (Reference 3). On metal parts, the technique was limited to surface temperatures below 800 K for lack of a stable thin film insulating layer to provide reliable electrical isolation from the base metal at higher temperatures. Layers of quartz, SiO and Al<sub>2</sub>O<sub>3</sub>, deposited by either vacuum evaporation or sputtering, were found to be too brittle to withstand the severe thermal strains (up to 500 kpsi) induced by the mismatch of temperature coefficients of expansion between the insulating layer and base metal. The work at Pratt & Whitney Aircraft is shown in Table I. The work of Dils, (columns 1 and 2), was performed on solid FeCrAlY test pieces on which a layer of aluminum oxide was furnace-grown. The thermocouple legs were then deposited on this insulator and tests to 1350K were performed. This combination of fabrication methods and materials was able to withstand these high temperatures.

In furnace tests on flat specimens (column 3), a typical turbine blade material (MAR-M-200+Hf) was coated with a typical turbine blade protective material (NiCoCrAlY); then Pt/Pt10Rh thermocouples were deposited on the furnace-grown Al<sub>2</sub>O<sub>3</sub> layer and tested to 1250K to demonstrate the feasibility of use on standard engine hardware. Strain gages were also tested (column 4) and erosion samples were prepared and tested (column 5) to further evaluate possible applications and assess potential problems. The strain gage tests demonstrated the feasibility of miniaturization of instrument patterns down to line widths of 75  $\mu$  m and the erosion tests proved the capability to thin film metal coatings to survive under engine conditions without prohibitive deterioration. Finally, an engine test of thin film thermocouple devices was performed with sensors mounted on turbine vanes (col. 6). Although problems occurred with the thin-film-to-lead wire connections, the sensors on the vanes survived engine operating conditions for 60 hours in most cases.

TABLE I

REVIEW OF PMA EXPERIENCE WITH SPUTTERED THIN FILM SENSORS  
ON MCrAlY SUBSTRATES AT HIGH TEMPERATURES

Item No. Date	1 1972-75	2 1975	3 9175-76	4 1976	5 1976	6 1977
Type of Sputtered Sensor	Thermocouples	Thermocouples	Thermocouples	Strain Gage	Erosion Samples	Thermocouples
Sputtered Film	Pt/Pt 10 Rh	Pt/Pt 10 Rh	Pt/Pt 10 Rh	Platinum	Platinum	Pt/Pt 10 Rh
Substrate Coating	- - -	- - -	NiCrAlY	NiCrAlY	NiCrAlY	NiCrAlY
Base Material	FeCrAlY	FeCrAlY	MAR-M-200 + Hf	Hastelloy X	B1900 + Hf	B1900 + Hf
Leadwire to Film Connection	Strap weld	Strap weld	Fire Platinum paste	Fired Platinum paste	None	Fired paste.
Configuration	Erosion bars, rods & airfoils	Cylinder	Flat bar	Strain bar	J79D 1st turbine blades	J79 2nd Turbine Vane
Test Facility	Lab combustor	Lab combustor	Lab furnace	Lab furnace	Operating engine	Operating Engine
Time Above 1250K, Each Sensor	100 hours	180 hours	170 hours	32 hours	20 hours	****
Cycles to 1250K, Each Sensor	100	20	6	1	6	****
Reference Publications	(4, 5)*	- - -	- - -	- - -	- - -	- - -
Condition at End of Test	Good**	Good**	Good**	Good**	Good***	Good*****
Remarks	20 specimens tested	Instrumented specimen for proof of calibration stability (see Fig. 3-6)	Instrumented specimen for proof of calibration stability	Strain test specimen	Engine erosion test	Metal Temp & Heat Transfer Coefficient



## 1.2 Objective

A three phase program has been undertaken by Pratt & Whitney Aircraft under contract to NASA-Lewis Research Center to establish the technology for making turbine blade temperature measurements using thin film temperature sensors. The ultimate goal is to develop a technique for producing thin film sensors directly on the blades and to demonstrate the performance of the sensors under actual engine operating conditions. The objectives of the first phase, completed under Contract NAS3-20768 and reported here, were as follows:

- o Perform a materials compatability study with four turbine blade and vane alloys and two MCrAlY protective coatings
- o Develop a fabrication procedure for thin film thermocouple elements
- o Develop a reliable lead-wire-to thin film connection technique
- o Fabricate complete sensor systems on simulated turbine blades
- o Test the sensor systems, including oven calibrations, vibration tests, and extended steady state and cycling tests to 1250K' in low velocity hydrocarbon gas flows

(An additional objective was added to the contract when problems arose during the testing phase. The objective was to study the mechanisms of adhesion between metal films and oxide insulations to determine ways of improving film adhesion).

The objectives of phase II are as follows:

- o Determine the best method to be used to improve adhesion of the thermocouple films on the oxide insulator
- o Apply the technology developed in phase I to the installation of a thin film temperature sensor on a turbine blade
- o Miniaturize the sensor slightly
- o Adapt the lead-wire-to-thin film connector to the turbine blade
- o Extend the test conditions to higher temperatures at the thin-film-to-lead-wire connection and higher velocities in the exhaust gas flow

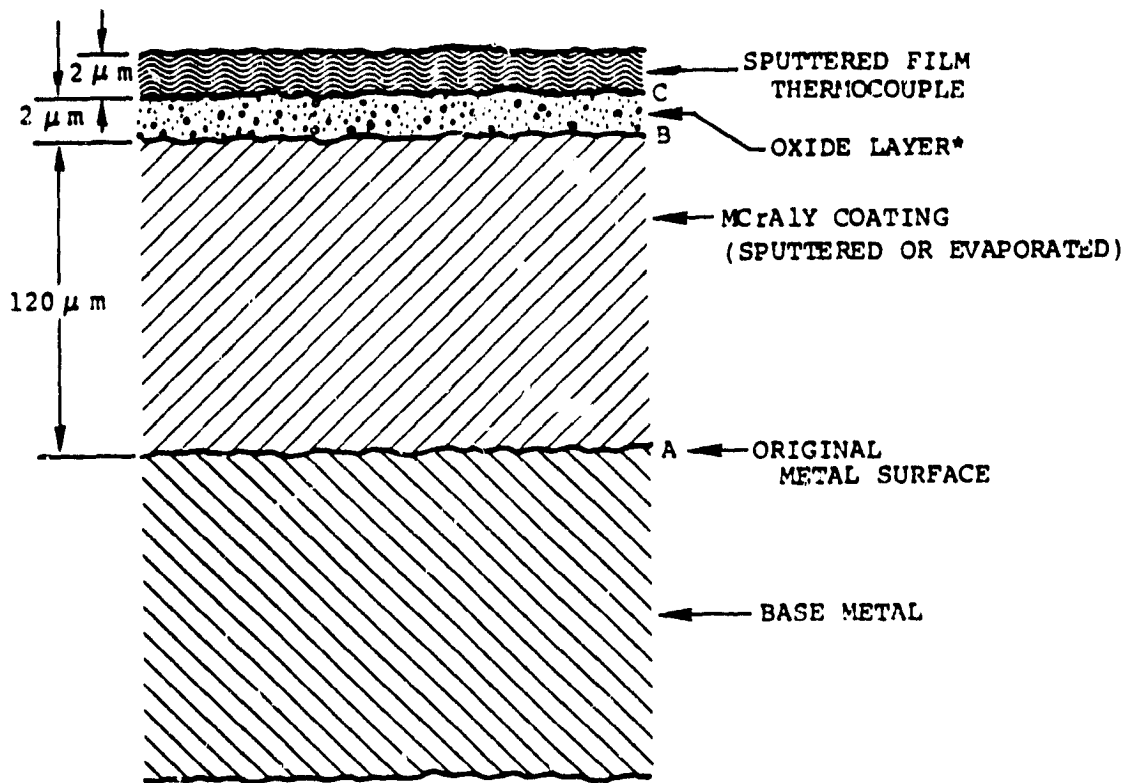
The objectives of phase III are as follows:

Test sensor systems on actual engine rotating turbine blades, with intercomparison of three measurement techniques; optical pyrometer, wire thermocouple, and thin-film thermocouple. Test conditions include metal surface temperatures up to 1250K, blade tip speeds up to 400 m/s, wheel diameters up to 95 cm, centripetal accelerations up to 35 kg, ten start-up and shutdown cycles, and 50 hours of total engine run.

The goals throughout the three phases of the program are: 75 percent survival rate for the 50-hour steady-state portion of the test program,  $\pm 1.2$  percent initial calibration accuracy of a thin film thermocouple, and drift rates of less than 4 percent in 50 hours from the initial value.

## 2.0 TECHNICAL APPROACH

The thin film thermocouple structure selected is illustrated in Figure 1. A section through one leg of the thermocouple is shown.



\*THE STABLE ADHERENT  $\text{Al}_2\text{O}_3$  INSULATING LAYER IS OBTAINED BY AT LEAST 50 HOURS OXIDIZATION ( $1300^\circ\text{K}$ ) OF THE COATING, FOLLOWED BY  $\text{Al}_2\text{O}_3$  SPUTTERING

Figure 1 Thin Film Thermocouple Cross-Section

The thermocouple legs are platinum and platinum-10 percent rhodium (Type S). This couple is designated Type S by ANSI Standard MC 96.1 and is metallurgically the simplest of those recommended for service up to 1800 K.

The key ingredient in the structure shown in Figure 1 is the alumina forming "MCrAlY" coating. The coating composition is typically 18 percent Cr, 12 percent Al, 0.5 percent Y, and the balance "M", where "M" is selected for best compatibility with the turbine blade material.

"M" may be Fe, Ni, Co, or a combination of Ni and Co. The attractive property of this coating is that at high temperatures in air, a dense layer of  $\text{Al}_2\text{O}_3$  forms on the surface. When properly grown and filled (by sputtering an additional amount of  $\text{Al}_2\text{O}_3$  onto the surface), this  $\text{Al}_2\text{O}_3$  coating is an excellent insulating material with high dielectric breakdown voltage. In addition, this oxide layer is mechanically tough and adherent, resisting erosion and spalling through extended temperature cycling and exposure to high speed contaminated gas flows. When the coating eventually spalls or erodes, a new protective oxide soon grows to take its place. It is this property that provides extended corrosion protection. The useful life of a thin film sensor sputtered onto the coating ends when the first spalling occurs.

The MCrAlY coatings when properly formulated are ductile, so that severe mechanical and thermal strains are not transmitted to the hard oxide layer. The strains within the  $\text{Al}_2\text{O}_3$ , therefore, remain within the elastic and buckling limits.

The strong bond at "B" in Figure 1 between the oxide layer and the MCrAlY material has been the subject of extensive study (Reference 7) and may be explained by the presence of the yttrium which combines with other constituents of the coating to form yttride "pegs" extending into the grain boundaries of the coating.

The bond at "C" in Figure 1, between the oxide layer and the noble metal of the thin film thermocouple, is not inherently strong because the platinum and platinum-10 percent rhodium sensor films do not chemically react with or chemically bond to  $\text{Al}_2\text{O}_3$ . In order to obtain an adherent sensor film, a high energy vacuum sputtering process (Figure 2) is employed that mechanically embeds the sensor metal molecules in a slightly roughened oxide surface. The sensor is ductile compared with the  $\text{Al}_2\text{O}_3$  and the sensor temperature coefficient of expansion matches that of  $\text{Al}_2\text{O}_3$  reasonably well. Therefore, the sensor is expected to withstand temperature cycling stresses with only a gradual long term shift in electrical resistance and an even smaller change in thermal emf (thermocouple output voltage).

The bond at "A" in Figure 1, between the MCrAlY coating and the turbine blade material is partially chemical in nature, and is enhanced by heat treatment to promote diffusion and solid solution in the interface region.

The original work of Dils and Follanabee (Reference. 4, 5 and Table I, columns 1 and 2) in the Combustor Materials Group at P&WA had thoroughly identified the physical properties of the materials used, and demonstrated in bench combustor tests the excellent durability and calibration stability of the proposed thin film thermocouple system when fabricated on thick solid bars of FeCrAlY materials.

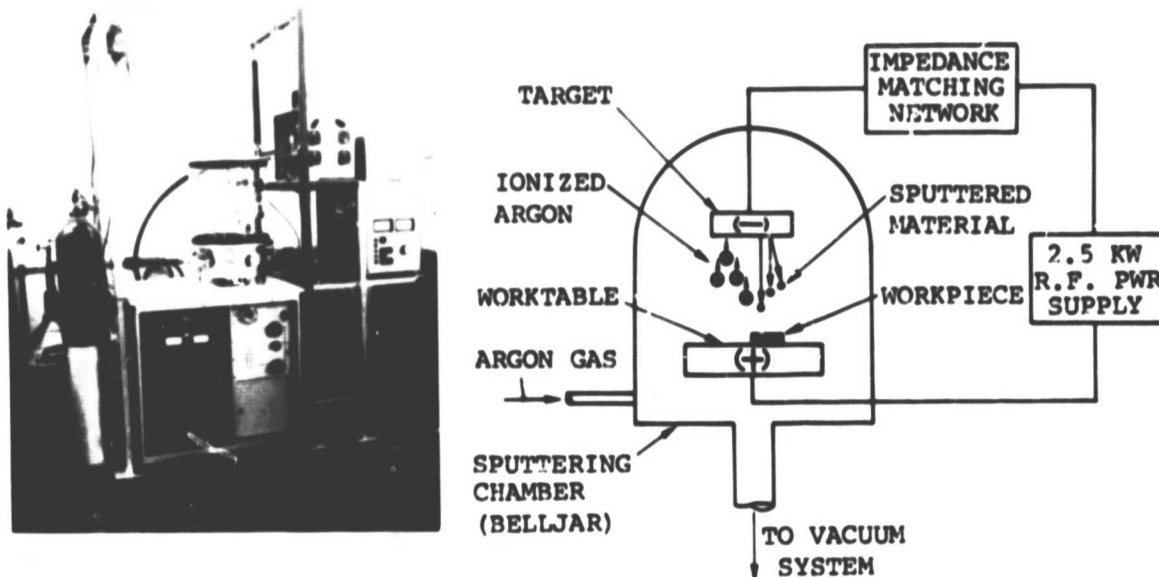


Figure 2 Sputtering Apparatus

This technology was adopted by the present investigating team in the Instrumentation Development Group at P&WA. In attempting to apply the techniques to the surfaces of thin MCrAlY coatings on turbine blades, it was found that special attention to surface finish before and after application of the MCrAlY coating, described later, was necessary to achieve a durable alumina layer on turbine blades and vanes (Table I, column 3).

No overcoating of the thin film thermocouples was planned because platinum was found to be sufficiently resistant to corrosion and erosion from an engine experiment (Table I, column 6). In this previous test at P&WA, platinum films sputtered on the oxidized NiCoCrAlY coated airfoil surface of first turbine blades were found to be in good condition when removed from the engine after 150 hours of operation at 1280 K (Table I, column 5). Platinum can in principle catalyze local surface combustion reactions in unburned hydrocarbons at high temperatures, and overcoating with an inert material seemed desirable for this reason. However, in combustor tests with platinum coatings on solid FeCrAlY bars no evidence of catalytic reaction had been found under simulated engine operating conditions. The possible benefits of an overcoating did not seem to justify the possible new problems of adherence and stability.

ORIGINAL PAGE IS  
OF POOR QUALITY

In the engine test of sample sputtered films, lead wire connections had been fabricated by oversputtering the sensor lead films onto lead wires embedded in insulated platform holes, and reinforced by application of fired platinum paste (Engelhart Industries No. 6869). These lead-wire connections failed early.

It remained to demonstrate that the thin film thermocouple system could be reproducibly fabricated on the surface of thin MCrAlY coatings on production turbine blades, that lead wires could be reliably attached, and that the system could be operated successfully in the engine environment.

### 3.0 APPARATUS, FABRICATION, AND TEST PROCEDURES

#### 3.1 Preliminary Fabrication and Test Procedures

The purpose of this phase of the program was two-fold: (1) to evaluate the compatability of various turbine blade and vane alloy materials with selected MCrAlY coatings used for protection of these materials and (2) to determine the suitability of these alloy-coating combinations to the various steps involved in the fabrication and testing of thin film thermocouple sensor systems.

Four turbine blade materials were chosen because they represent materials commonly used in jet engine turbine blades and vanes.

- 1 IN 100 - cast nickel-based alloy
- 2 MAR-M-509 - cast cobalt-based alloy
- 3 B-1900 + hafnium - cast nickel-based alloy
- 4 MAR-M-200 + hafnium - cast nickel-based alloy

Alloy compositions are summarized in Table II.

TABLE II

PRELIMINARY FLAT PLATE TEST PIECE MATRIX

Composition of Blade and Vane Materials Percent				
Element	MAR-M-509	B1900 + Hf	In100	MAR M200 + Hf
Ni	10	63	61	59
Cr	23	8	9	9
Co	55	10	15	10
Ti	0.2	1	5	2
Al		6	6	5
Mo		6	3	
C	0.6	0.1	0.2	0.1
W	7			12
Ta	3.5	4.2		
Zr	0.5		0.06	
Ba		0.01	0.01	0.01
Hf		1.1		2
V			1	
Nb				1

The initial developmental test piece was 2.5 cm wide by 5 cm long by 0.3 cm thick. Five pieces of each material were cast. Four pieces of each material were machined in the manner shown in Figure 3a and the remaining piece of each material was machined as in Figure 3c. The grooves and holes were used to test different thin-film-to-lead-wire connectors.

On the advice of the Coating Materials Group at Pratt & Whitney Aircraft, two candidate alumina forming coatings were selected for trial on all four turbine blade and vane materials:

1. NiCoCrAlY (Ni-23Co-18Cr-12Al-0.3Y) (PWA 270), considered the most compatible with the nickel-based alloys.
2. CoCrAlY (Co-19Cr-12Al-0.4Y) (PWA 68) considered most compatible with the cobalt-based alloys.

The twenty test pieces were separated into five groups, each group containing one piece of each material, as shown in Table III. Three groups of test pieces were coated with NiCoCrAlY and two groups were coated with CoCrAlY. One group was machined with countersunk holes (Figure 3c), for the purpose of experimenting with bolt-down lead wire connections. Four groups were machined with grooved areas (Figure 3a) to evaluate various recessed thin film-to-lead-wire connections. The thin films of thermocouple material were deposited on the test pieces in the patterns shown in Figures 3b and 3d.

TABLE III

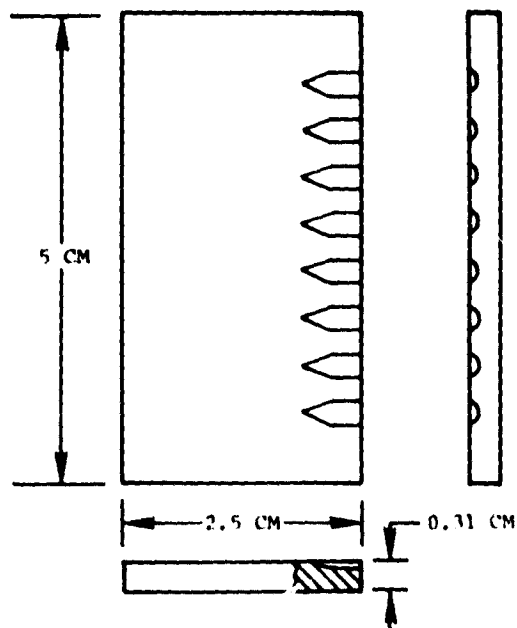
PRELIMINARY FLAT PLATE TEST PEICE MATRIX

Group	1	2	3	4	5
Material*	1 2 3 4	1 2 3 4	1 2 3 4	1 2 3 4	1 2 3 4
Coating	NiCoCrAlY	NiCoCrAlY	NiCoCrAlY	CoCrAlY	CoCrAlY
Configuration	Grooves	Holes	Grooves	Grooves	Grooves

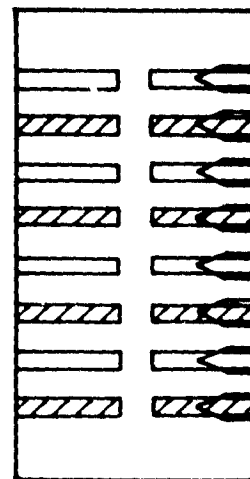
Material Code:

- 1 - MAR-M-509 (PWA 647)
- 2 - B1900 + Hf (PWA 1455)
- 3 - IN100 (PWA 658)
- 4 - MAR-M-200 + Hf (PWA 1422)

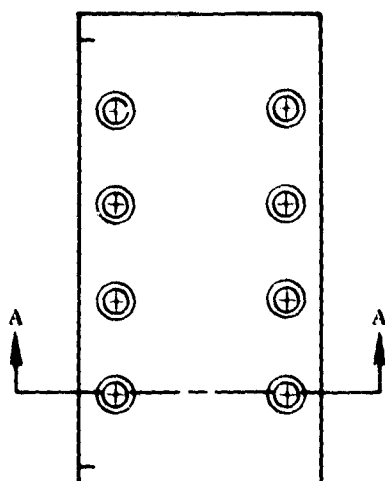




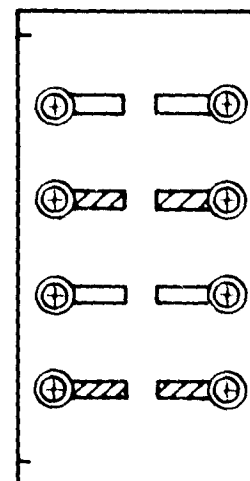
a. GROOVED TEST PIECES



b. GROOVED TEST PIECES WITH THIN FILM THERMOCOUPLE MATERIAL



c. TEST PIECE WITH COUNTERSUNK HOLES



d. TEST PIECE WITH COUNTERSUNK HOLES AND THERMOCOUPLE MATERIAL

0.127 CM. PLATINUM FILM

0.152 CM. PLATINUM-10% RHODIUM FILM

Figure 3 Flat Plate Test Pieces

The basic fabrication procedure is outlined in Table IV. A narrative description of each step is provided here for a clear understanding of the principal requirements in fabricating thin film thermocouple systems on coated turbine blades.

TABLE IV  
OUTLINE OF FABRICATION PROCEDURE FOR  
THIN FILM THERMOCOUPLE ELEMENTS

1. Polish and clean the turbine blade material surface
2. Vapor hone
3. Electron beam vapor deposition coat with MCrAlY
4. Dry glass beadpeen the coating
5. Polish the coating
6. Grit blast the coating
7. Heat treat at 1350K 4 hours in dry hydrogen
8. Oxidize in air at 1300K for a minimum of 50 hours
9. Sputter  $Al_2O_3$
10. Age at 1250K for 1 hour
11. Mask for platinum sputtering
12. Sputter platinum
13. Mask for platinum 10 percent rhodium
14. Sputter platinum 10 percent rhodium

1. After casting and machining, the twenty test pieces were mechanically polished on one side to a surface finish of  $0.25 \pm 0.1$  micrometers measured on a Talysurf profilimeter.

All test pieces were then degreased in methylene chloride, cleaned in an ultrasonic Alconox detergent bath, rinsed in boiling deionized water until no detergent residue remained, rinsed in hot isopropyl alcohol, soaked in a hot ultrasonic Freon 12 bath, and given a final hot freon vapor rinse. After cleaning, the test pieces were handled with cotton or nylon gloves to prevent oil or grease contamination, and were stored in a dessicant chamber between operations.

2. Each piece was vapor-honed (grit-blasted with a water spray) just before coating.
3. A  $120 \mu m \pm 24 \mu m$  MCrAlY coating was then applied by the electron beam vapor deposition process, by evaporation from a molten pool of the coating material in a vacuum chamber. The test pieces were rotated during the coating cycle.
4. The finished coating was dry glass bead peened to increase its density.

5. The coating surface was repolished mechanically to a  $0.25 \pm 0.1 \mu\text{m}$  finish.
6. The surface was then lightly grit blasted (320 grit  $\text{Al}_2\text{O}_3$  at 150 to 300 kPa pressure at about 45 degree incidence angle and 8 cm distance) to produce a controlled surface roughness for adherence of platinum films. (The grit blasting does not change the measured arithmetic average roughness, but alters the texture from a mirror like surface to a dull gray). The entire cleaning procedure was repeated after polishing and again after grit blasting.
7. The test pieces were then heat treated at 1350 K (1975°F) in dry hydrogen at a pressure of 100 kPa for four hours. The environment during this hydrogen heat treatment is extremely critical to the ultimate success of the thin film sensor system. The purpose is to stabilize the coating, to start the migration of aluminum toward the surface, and to start the gradual growth of a dense, hard, and adherent layer of  $\text{Al}_2\text{O}_3$  in an oxygen-poor environment. The partial pressure of oxygen should be below  $10^{-5}\text{Pa}$ . Excessive oxygen results in the appearance of poorly adherent blue oxides of chromium and cobalt, as well as spinels (Cr-Al-O compounds). It is believed that an argon atmosphere or a vacuum would produce as good a result as hydrogen, but these alternatives were not explored in this program.

Contamination by more than 0.1 ppm of gaseous water, chlorine, sodium, or hydroxyl radical during the heat treatment can result in a poor  $\text{Al}_2\text{O}_3$  structure such as the stringy reticulated whiskers of low adhesion described in Reference 9.

After completion of the heat treatment, small samples were cut from eight test pieces, including representative samples of each coating on each of the four materials. The samples were microsectioned and metallography was performed using an electron microscope to determine the thickness and structure of the coatings.

8. All test pieces were cleaned in a Freon 12 rinse and oxidized at 1300 K for 50 hours in air in a clean oxidation furnace. The furnace used was a new Marshall oven with high-purity aluminum oxide muffle, dedicated to this oxidation process and never used for any other purpose. The test pieces were then evaluated for oxide insulation quality as follows:
  - a. A measurement of the electrical resistance across the insulating films was made at randomly selected points.
  - b. A measurement of the dielectric breakdown voltage in areas that were not covered later with thin films was performed.
  - c. A qualitative measurement was made of oxide hardness (ease of penetration with an electrical probe).

- d. A visual examination was performed with a 200X optical microscope to evaluate surface grain size, color, structure, whiskers, or cracks.

If the electrical resistance of the insulative film was found to be less than  $10^6$  ohms on any sample, the sample was returned to the oxidation furnace for an additional oxidation period of 25 hours at 1300 K. After the additional oxidation period, the test pieces were re-evaluated. Further oxidation, if required, was made in 25 hour segments to a maximum of 150 hours for any test piece.

9. Selected test pieces that successfully passed the insulating film evaluation test were cleaned in a Freon 12 rinse and sputtered on one face only with 1.0 to 1.5  $\mu\text{m}$  of  $\text{Al}_2\text{O}_3$ . A Materials Research Corporation 15 cm diameter MARZ grade  $\text{Al}_2\text{O}_3$  planar target (99.992 percent purity) was used and the sputtering was done in an r.f. diode sputtering system at 1100 VDC (self bias), 15 cm spacing, for about 9 hours in argon-5 percent  $\text{O}_2$  gas mixture at  $5 \times 10^{-1}$  Pa. Test pieces were sputtered in groups of four. The work pieces were initially sputter etched for 5 minutes to clean the surface.
10. After sputtering, each test piece was aged at 1250 K for one hour to assure the formation of  $\alpha$ - $\text{Al}_2\text{O}_3$  structure in the sputtered  $\text{Al}_2\text{O}_3$ .
11. The test pieces were then masked for platinum film, using the tape plus positive photoresist method. Strips of 3M No. 218 tape were applied directly to the surface to cover areas which would become platinum films. The entire surface was then painted with liquid photoresist (Shipley No. AZ-1350-J), a material which hardens to a protective layer when baked at 470 K, but which can be easily removed with a solvent later. After baking, the tape was removed to expose the stripe pattern. The surface was then ultrasonically cleaned in a Freon 12 bath at room temperature to remove traces of tape residue. The Freon 12 ultrasonic bath temperature was raised to 320 K and the cleaning was continued (for several hours in some cases) until a water break test indicated no residue. In the water break test, deionized water is placed on the surface. If it flows into a film over the entire surface, with no breaks, the cleanliness is acceptable. Later in the program, during fabrication of thin film thermocouples on simulated blades, this cleaning procedure was found to be critical to success, since any tape residue severely degraded the adherence of the platinum films.
12. Platinum was then r.f. diode sputtered onto the selected test pieces to a thickness of 2.0  $\mu\text{m}$  using a 15 cm, diameter 99.98 percent pure platinum plane target in a pure argon gas at  $5 \times 10^{-1}$  Pa at 800 VDC, 15 cm. spacing for 4.5 hours. The work pieces were initially sputter etched for 5 minutes. After sputtering the

photoresist was removed by washing with a solvent. Remaining traces of photoresist were removed by charring in an oven. The resistance of each platinum film to the base material was measured. The test pieces having 25 percent or more of the platinum films showing less than  $10^6$  ohms resistance to the base material were re-oxidized in the oxidation furnace at 1300 K for 25 hours. When the test piece was acceptable, the film resistance was measured.

13. and 14.

All test pieces with sputtered platinum films that were accepted were remasked and sputtered with platinum-10 percent rhodium films to the same thickness range as the platinum films, using thermocouple quality target material. All sputtering parameters were the same as those used for platinum. and the same resistance-to-ground value was used to determine the need for reoxidation. Film resistance was measured.

Clean glass slides were included with each group of test pieces sputtered to provide material for chemical analysis of the sputtered platinum-10 percent rhodium films.

All films were then tape tested for adherence, using Dodge Industries No. 2045-5 tape pressed firmly in place and then removed by pulling vertically. If more than 1 percent of the film area was removed, the film adherence was judged not acceptable.

Each accepted test piece was then subjected to furnace tests in which the test piece was cycled 20 times from room temperature to 1250 K, by plunging the piece into a preheated furnace, soaking one hour, and removing the piece from the furnace (air quench). After completion of the furnace environment tests, tape tests, and resistance measurements of all films and their resistances to the base material were repeated. The surfaces were again examined with a 200X optical microscope.

Insulation resistance measurements vs temperature from 300 K to 1250 K were carried out on one sample (No. 35).

### 3.2 Thin Film-to-Lead-Wire Connection Fabrication

Lead wire attachment experiments were carried out on the flat plate specimens of Figure 3 and a successful hot compression bonding technique was evolved.

Four methods of joining 0.075 mm wires of platinum and platinum-10 percent rhodium to thin films of the same material were evaluated: ultrasonic welding, laser welding, bolted connections, and hot compression bonding. Fired conductive pastes were considered but not tested in this program because the previous experience in a full scale engine test (described earlier) was not encouraging.

Ultrasonic welding uses high frequency vibration plus pressure to form a weld. Samples of platinum-10 percent rhodium thin films and wire were sent to several vendors that specialize in the manufacture of wire-to-thin film bonding machines for the microelectronics industry. These machines are primarily designed to weld soft wires such as gold or aluminum to microelectronic chip wire connection pads.

Laser welding is routinely used at P&WA for joining fine wires to fine wires.

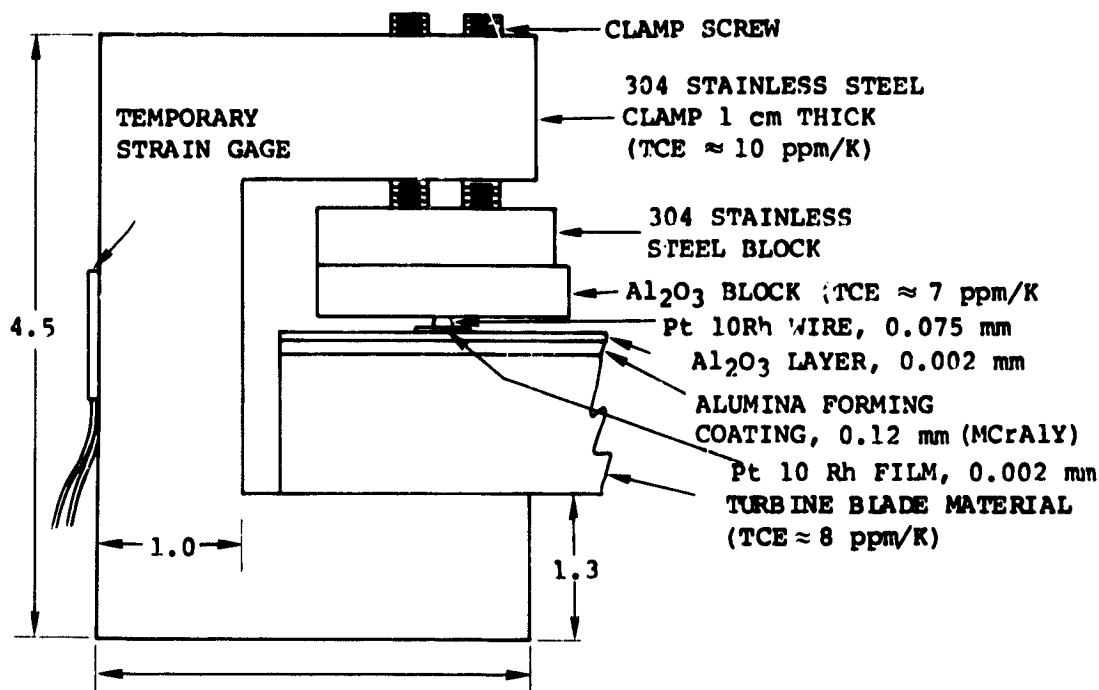
To fabricate a bolted connection the test pieces shown in Figure 3c were used. Each film of a sputtered thermocouple was sputtered down into the insulated countersunk hole, as shown in Figure 3d. A flat head, platinum coated, 6-32 stainless steel bolt was placed into the countersunk hole and tightened with a nut. A lead wire tack welded to the head of the bolt completed the connection.

Hot compression bonds are formed by application of a large force at a high enough temperature (below the melting point of the materials to be bonded) for a long enough time to produce interdiffusion of the materials. (A D.C. voltage is sometimes applied to form a "field-assisted bond"). The technique has long been used to join soft metals together (e.g., Reference. 8) but a successful application has not previously been reported using hard alloys (e.g., platinum-10 percent rhodium).

The apparatus used to form hot compression bonds is sketched in Figure 4. A photograph of four bonds being formed simultaneously is shown in Figure 5. A detailed view of the resulting bonds is shown in Figure 6.

The essence of the process is to force the two materials together until they are plastically deformed and then heat the assembly in a furnace until a bond is formed. Plastic deformation ensures intimate contact at the interface and rupture of surface oxides on the wire-film interface so that clean surfaces are in contact. Reference 26 shows scanning electron microscope microphotographs of Al-Al bonds in which the break-up of the hard oxide is clearly evident.

In Figure 4, the wire is clamped against the thin film with a force sufficient to result in about 50 percent deformation of the wire without fracture of the supporting insulating oxide. During application of the clamping force, the electrical resistance of the leadwire to ground (substrate) must be continuously monitored, using a low voltage ohmmeter. The clamping force must be reduced if a sudden decrease in electrical resistance is observed. It was found that if the leadwire resistance to ground decreases to a few ohms (indicating fracture of the insulating layer), the low resistance is permanent and cannot be repaired by further heat treatment up to 75 hours at 1300 K.



\*TCE = TEMPERATURE COEFFICIENT OF EXPANSION

Figure 4 Diffusion Bonding Apparatus - All Dimensions are in centimeters (not to scale).

A clamp instrumented with a strain gage (Figure 4) was calibrated and used to determine a typical clamping force. The force measured for a typical bonding run was about 530 N (120 lbs) applied to two platinum-10 percent rhodium lead wires. The calculated stress in each 0.075 mm x 1 cm area was therefore about 350,000 kN/m<sup>2</sup>, which is approximately the yield strength of annealed platinum-10 percent rhodium. No change in lead wire resistance to ground was noted at this clamping pressure. The resistance remained above 20 megohms (the limit of instrument).

To distribute the clamping force over several lead wires, a strip of stainless steel was placed under the clamp screws. A hard, dense smooth strip of Al<sub>2</sub>O<sub>3</sub> was placed between the lead wires and the stainless steel strip to eliminate wire sticking and possible metallurgical reactions with the stainless steel.

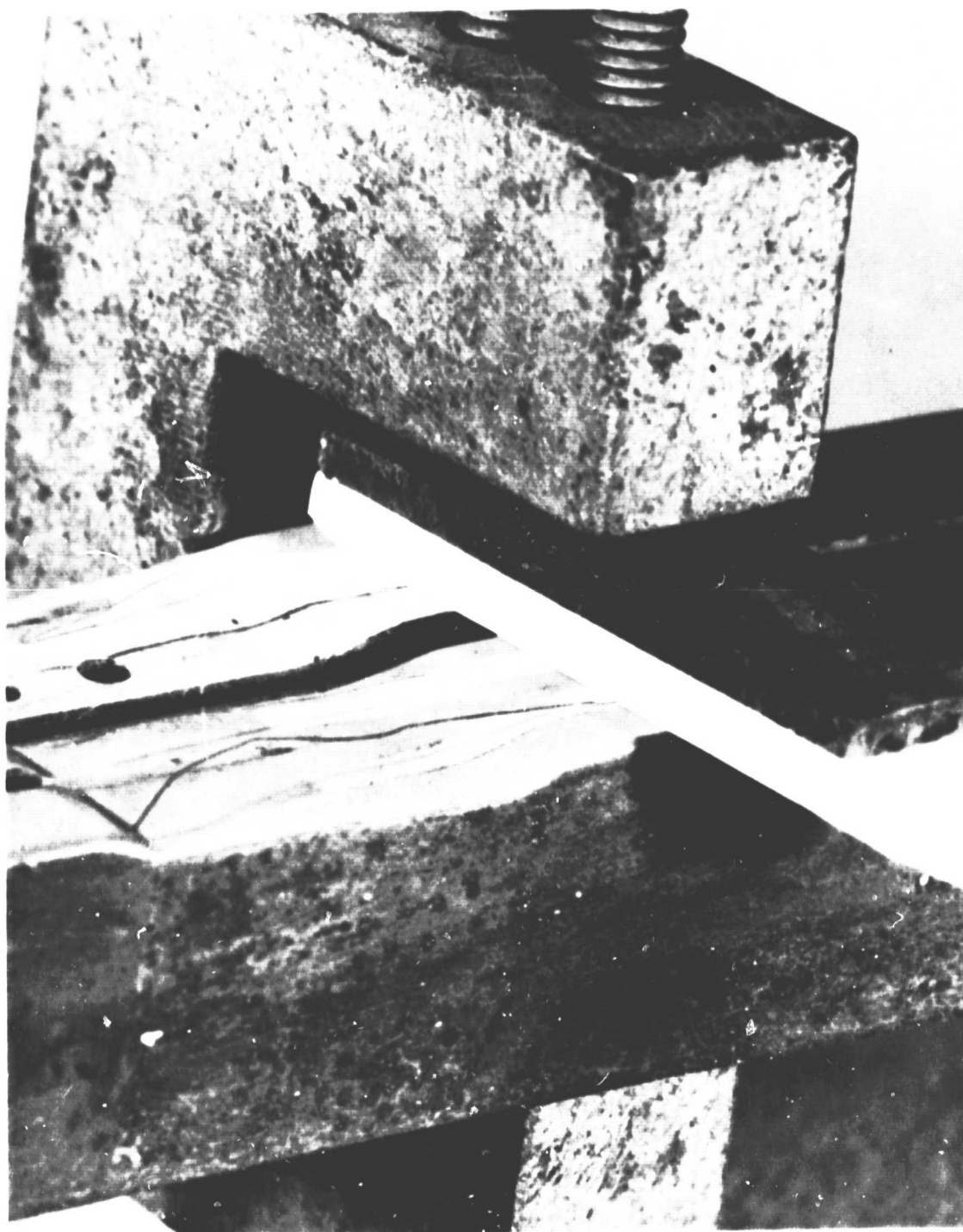


Figure 5 Lead Wires (0.075 mm diameter) - The lead wires are shown clamped to the thin films on the simulated blade in preparation for diffusion bonding.



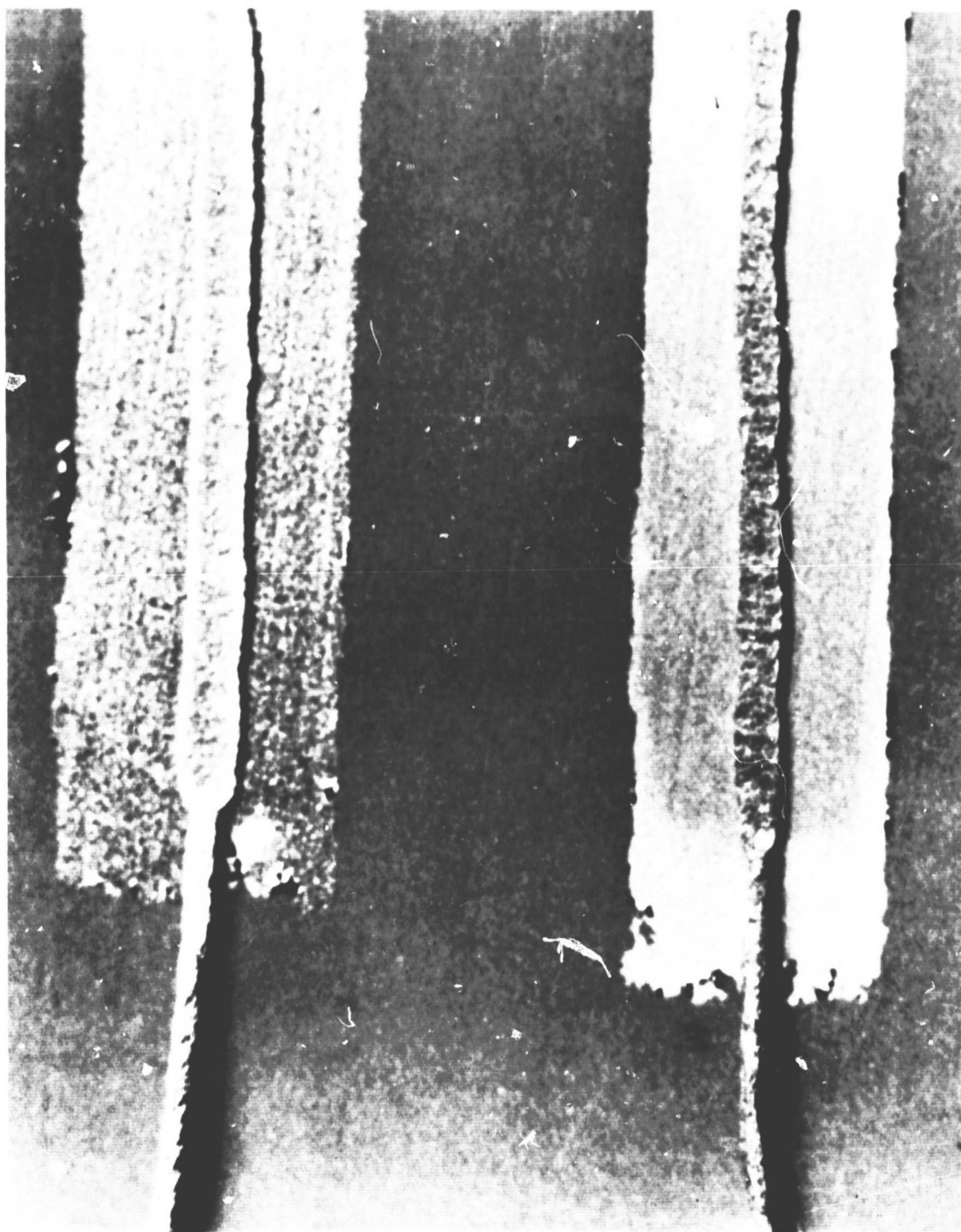


Figure 6 Completed Diffusion Bonds of 0.075 mm Platinum and Platinum-10 Percent Rhodium Lead Wires to Thin Films on a Simulated Blade

### 3.3 Fabrication of Thin Film Thermocouples on Simulated Turbine Blades

Eight simulated turbine blades were fabricated, each with two thin film thermocouple sensor systems and five reference wire thermocouples. Figure 7 is a drawing of a simulated blade with the thin film thermocouple systems. The base material was cast MAR-M-200 plus hafnium. The simulated blades were channel shaped castings 18.1 cm long and 1.90 x 1.27 x 0.32 cm cross section. The left end of the blade was designated the thin film-to-lead wire connection end and grooved to accommodate recessed connections. One thin film thermocouple junction was located 15.6 cm from the connection end and one 11.4 cm from the connection end. Platinum and platinum-10 percent rhodium thin films extended from each junction to a point 2.5 cm from the connection end, where thin film-to-lead wire connections were made. Lead wire pigtails 2 cm long of 0.075 mm platinum or platinum-10 percent rhodium wire were hot compression bonded to the lead films. One end of a 60 cm length of 0.81 mm diameter platinum-10 percent rhodium sheathed dual thermocouple extension wire was strap welded to the surface 1 cm from the connection end of the simulated blade. Each extension wire contained two 0.127 mm conductors (one platinum and one platinum-10 percent rhodium) in

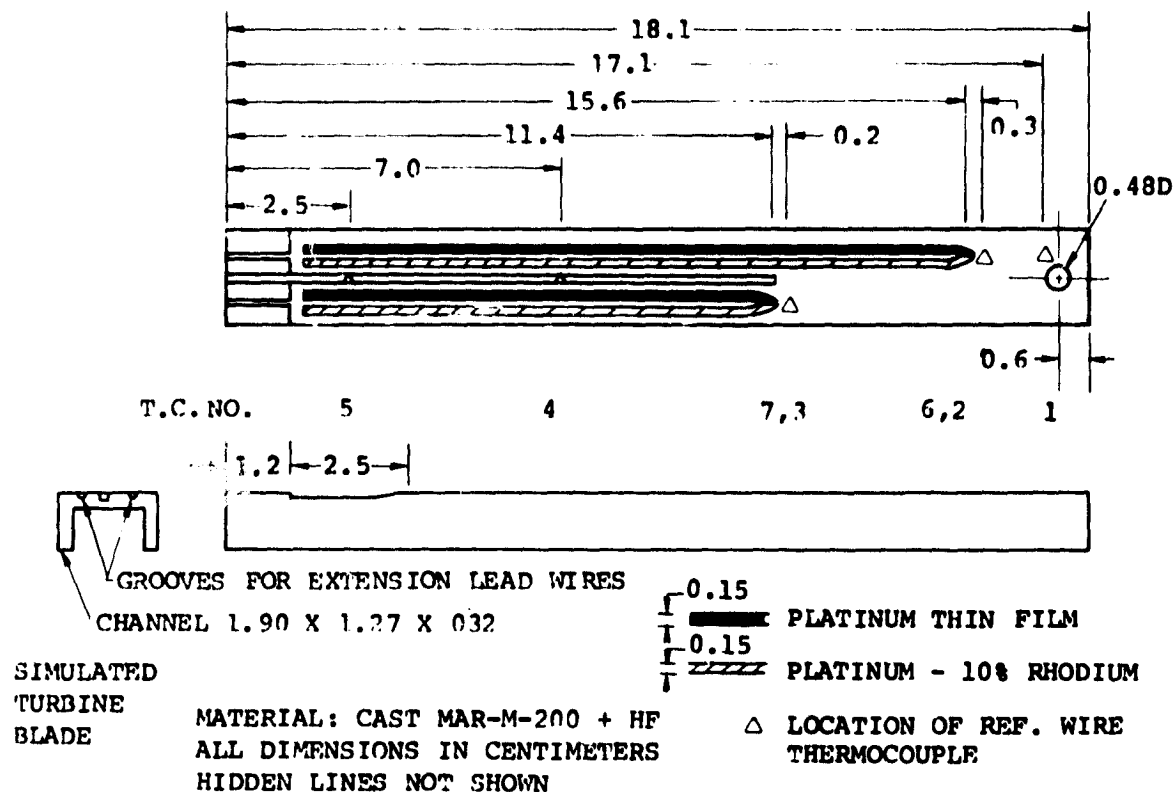


Figure 7 Layout of Simulated Turbine Blade with Thin Film Temperature Sensors - The locations of reference wire thermocouples are indicated.

magnesium oxide ceramic insulation. These two conductors were tweezer welded to the 0.075 mm pigtails of the thin film sensor system. The exposed lead wires were then embedded in ceramic cement (Cerama-Dip No. 538). A Harco thermocouple connector was used at the other end of the 60 cm sheathed cable to connect long Type S extension wires to a temperature recorder.

Five grounded Type S wire thermocouple junctions (formed from additional 60 cm lengths 0.81 mm diameters of high temperature sheathed cable) were spot welded at the locations shown in Figure 7 to provide reference measurements of surface temperature profile along the length of the simulated blade. The thermocouple wire used was of reference grade ( $\pm 2.5$  K accuracy at 1300 K).

The procedure for fabricating of the thin film thermocouple systems and lead wire attachments was the same as that used on the preliminary flat plate test pieces described in the previous sections except for the following refinements.

(1) After fabrication and lead wire attachment, the assembly was aged in air for one hour at 1250 K to stabilize the platinum and platinum-10 percent rhodium films because of a calibration drift that usually occurred during the first hour of operation.

(2) Initial oxidation time of the MCrAlY coating at 1300 K in air (step 8, Table IV) was held to the minimum 50 hours. Most specimens had adequate insulation resistance after this initial period. It was found that if the insulation resistance was over 100 ohms at this point, then the subsequent heat treatments associated with aging the sputtered  $Al_2O_3$ , lead wire bonding, and aging the platinum and platinum-10 percent rhodium films brought the resistance above 20 megohms. In this way during the fabrication procedure the total exposure time of the turbine blade material in air to temperatures in the 1100 K to 1300 K range was ordinarily below 75 hours.

The nomenclature of simulated blade serial numbers consists of a number, letter, and subscript, e g. 2L. The number and letter indicate the casting run and casting mold used, respectively. The subscript "1" indicates a virgin coating (less than 75 hours exposure above 1100 K during fabrication). The subscript "2" indicates a reworked specimen, in which part of the original coatings are stripped off and the pieces go through some of the steps of the fabrication process again.

Some simulated blades required reworking due to adhesion problems later in the program; total exposure was about 150 hours above 1100K in these cases. A photograph of a finished specimen is shown in Figure 8.



The object of these tests was to compare the output of the thin film thermocouple to that of its adjacent reference wire thermocouple. The temperature gradient was imposed on the thin film thermocouple to determine whether its calibration would match that of the reference wire thermocouple. Any discrepancies in the thin film thermocouple, such as variations in film composition along its length or leakage to ground through the  $\text{Al}_2\text{O}_3$  insulating layer, would in the presence of a temperature gradient, result in a temperature indication different from that of the actual junction temperature by an amount dependent upon the temperature gradient.

### 3.5 Vibration Test Equipment and Procedures

Vibration testing of two completely assembled simulated blades including extension leads, was performed using a commercial vibration apparatus having a sine wave force rating of 15500 N (3500 lbs. force) and a frequency range of 5 to 3000 Hz. The vibrational frequency was swept from 100 to 400 Hz at a rate of one octave per minute at 8 g peak acceleration. This test cycle was applied for one hour on each of three axes.

The fixture was a holding frame and a broach block was selected to conform with the simulated blade.

One simulated blade assembly (No. 4L<sub>1</sub>) was vibration tested before thermal testing and another (No. 4R<sub>1</sub>) after all thermal testing. Electrical continuity of the thin film sensor systems and electrical insulation resistance from thin film to base material were measured before and after the vibration testing.

### 3.6 High Temperature Exhaust Gas Test Equipment and Procedures

Four of the eight simulated blades (4L<sub>1</sub>, 4R<sub>2</sub>, 2R<sub>1</sub>, 3R<sub>1</sub>) were subjected to an exhaust gas environment in a simulated combustor. This facility created a nominal temperature profile on the simulated test blade as shown in Figure 9. The gas velocity was approximately 40 m/s. Due to difficulties, this portion of the tests lasted  $\approx 1$  hour per test piece. Following these tests, this facility was no longer available for use. The next four of the eight simulated blade assemblies (Nos. 2L<sub>1</sub>, 3L<sub>1</sub>, 4L<sub>2</sub>, and 2R<sub>2</sub>) were subjected to an exhaust gas environment test by exposing each specimen to an oxyacetylene torch flame in the following sequence:

- A. 50 hour steady state test with a nominal temperature profile as shown in Figure 10, including 10 cycles from this temperature profile to ambient temperature. The test sensor and reference wire thermocouple temperatures were monitored. Note that the maximum blade temperature at the center of the blade is 1250K.

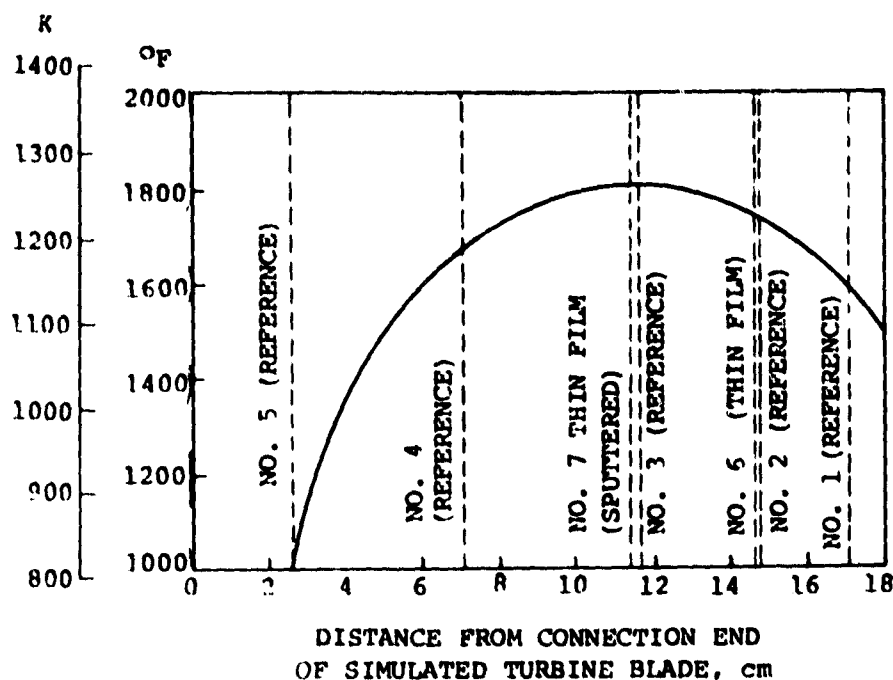


Figure 9 Nominal Temperature Profile Along The Simulated Turbine Blade During 1250 K Steady State Exhaust Gas Flow Tests - Dotted lines show thermocouple locations; Nos. 1 - 5, reference wire thermocouples, Nos. 6 & 7, thin film thermocouples.

- B. 20 cycles from room ambient to the nominal temperature profile (1250 K). Each cycle consisted of 20 minutes in the designated temperature profile followed by 20 minutes at room ambient for a total test time of 13 1/3 hours, with 6 2/3 hours at 1250K. The test sensor and reference wire thermocouple temperatures were continuously monitored.
- C. 1 hour steady state with the nominal temperature profile for a final calibration check. The test sensor and reference wire thermocouple temperatures were monitored.

Thus, unless failure occurred sooner, each of the four specimens was cycled 31 times from room temperature to 1250 K, and each spent a total of 57.7 hours at 1250 K.

The instrumentation for these tests was the same as that used in the oven tests. A continuous chart recording of all seven thermocouples (two thin film and five reference wire) was obtained. In addition, the readings of the two thin film sensors (Nos. 6 and 7) and the adjacent two reference wire thermocouples (Nos. 2 and 3) were measured and recorded every 10 minutes with the precision digital temperature indicator.

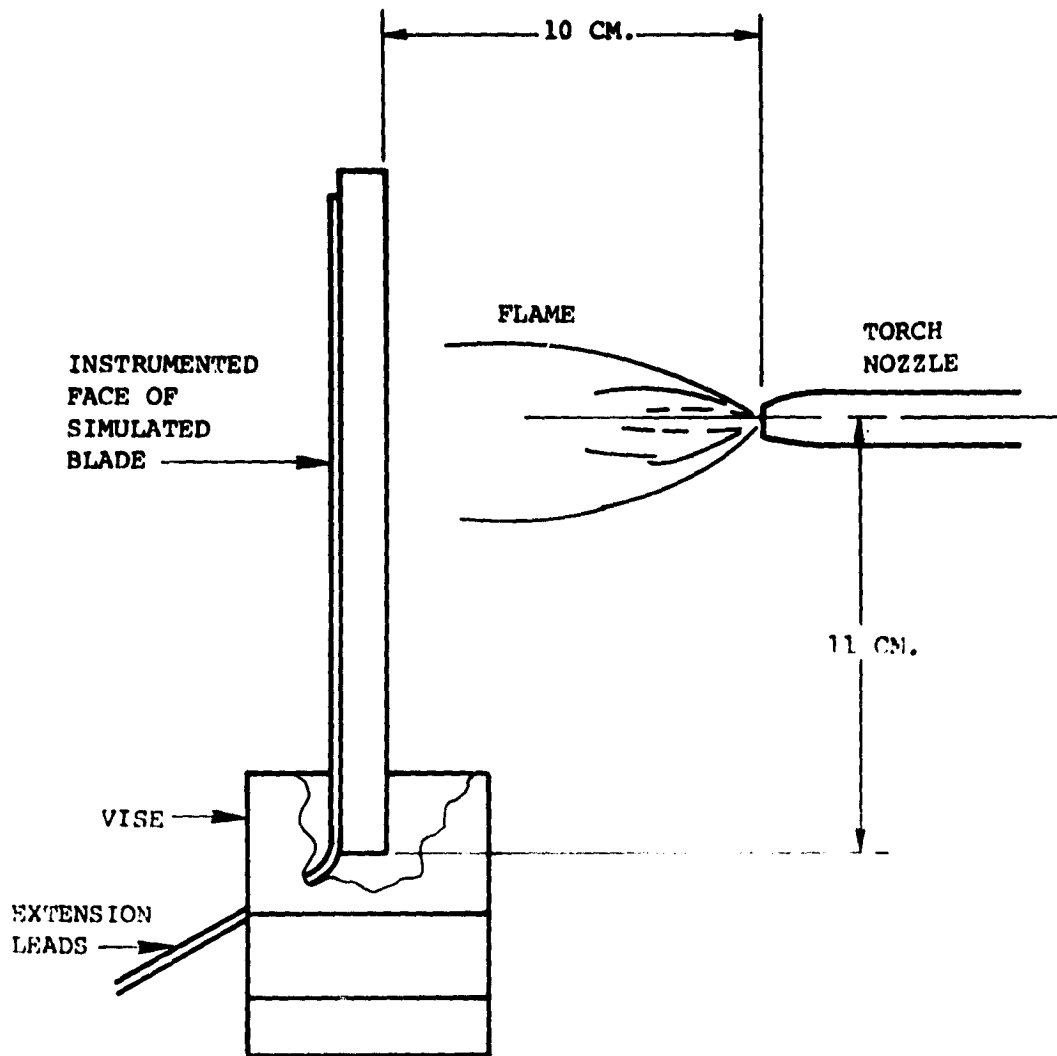


Figure 10 Oxyacetylene Torch Exhaust Gas Flow Test Setup

A drawing of the test setup is shown in Figure 10. The torch was held 10cm. from the simulated blade and directed at its rear surface, so that the thermocouple systems and leadwork on the surface were not exposed to visible radiation directly from the flame. A torch nozzle size was selected that produced the desired metal surface temperature profile (as indicated by the five reference wire thermocouples). Heat up and cool-down times were about five minutes.

After each temperature cycle, the connector at the free end of the 60 cm sheathed extension cable was disconnected and the resistances to ground and the thermocouple loop resistances were measured, using a low voltage ohmmeter Data Precision Model 175. On a few occasions these resistance measurements were recorded when the simulated blade was operating at maximum temperature.

One of these four tested simulated blades ( $2L_1$ ) and two others which were untested ( $6R_1$  and  $4L_2$ ) were delivered to NASA LeRC for independent evaluations.

The remaining simulated blade ( $6L$ ) was used to investigate a number of problem areas that were identified during the course of fabrication and initial test trials. These problem areas will be discussed in Section 4.0, Results and Discussion.



## 4.0 RESULTS AND DISCUSSION

### 4.1 Preliminary Tests

Test results are summarized in Table V. All 20 test pieces were initially coated and subjected to heat treatment. Eight of these specimens were then selected for metallographic work to evaluate the quality of the coatings at this critical point in the fabrication process.

Morphology of the coatings on these eight specimens is shown in Figure 11. Particularly notable is the uniform fine-grained ( $1\ \mu\text{m}$ ) structure with slight elongation of grains in the direction normal to the blade surface. The excellent structure is partly due to polishing before coating. In coatings applied to unpolished surfaces, vertical chimney-like defects had been noticed in the past. These defects are believed to be associated with "shadowing" in the vicinity of surface imperfections during the electron beam vapor deposition of the coating on rough surfaces. The outer layers of such chimney-structured coatings have been found to crack or spall easily during temperature cycling. The structures of Figure 11 are typical of durable coatings with adherent oxide formation.

Figure 12 shows composition profiles (of Ni, Co, Cr, Al, and Y) in the NiCoCrAlY coating after  $\text{H}_2$  heat treatment on Specimen No. 6L<sub>2</sub>, obtained by X-Ray dispersive analysis. Each photo in Figure 12 provides information on a single atomic species. A light area indicates a concentration of the particular species. Note that the Ni, Co, and Cr are uniformly dispersed through the coating. There is a high concentration of Al at the outer surface (top), presumably in the thin ( $0.1\ \mu\text{m}$ ) layer of  $\text{Al}_2\text{O}_3$  formed during heat treatment. This was expected, due to the presence of traces of  $\text{O}_2$  in the  $\text{H}_2$  furnace. There is an aluminum depleted layer just below the surface, about  $10\ \mu\text{m}$  thick, from which aluminum has migrated to the surface during the heat treatment. Yttrium (barely visible in Fig. 12) is concentrated at the interface between the surface oxide and the coating, where the yttride "pegging" of the oxide described in Section 2.0 takes place.

After oxidation in air at 1300 K for a long enough time (75 to 95 hours) to produce an oxide layer of resistance greater than 20 megohms, Table V shows that 50 percent of the specimens had developed a hard, dense oxide. About 75 percent passed this qualitative hardness test. Eleven pieces were selected, to include samples of NiCoCrAlY on all four base alloys and CoCrAlY on all four base alloys. After a further 25 hours of oxidation of 11 selected pieces all but one (a CoCrAlY on Ni based MAR-M-200 plus hafnium) showed a hard, dense oxide. Overall there seems little to recommend one combination of blade material and coating over another on this basis, though NiCoCrAlY is perhaps slightly preferable on the Ni based MAR-M-200 plus hafnium.

TABLE V

## FLAT PLATE RESULTS

Coating	NiCoCrAlY				NiCoCrAlY				NiCoCrAlY				CoCrAlY				CoCrAlY					
Configuration	Grooves				Holes				Grooves				Grooves				Grooves					
Sample No.	2	11	22	31	51	61	71	81	1	12	21	32	6	15	26	35	5	16	25	36		
Mat's Code*	1	2	3	4	1	2	3	4	1	2	3	4	1	2	3	4	1	2	3	4		
Coat + H <sub>2</sub> Heat Treat	X	X	X	X	X	X	X	X	X	X	X	X	X	X	X	X	X	X	X	X		
Metallography									X	X	X	X					X	X	X	X		
Oxidize 75 to 95 Hours	X	X	X	X	Xb	X	X	X	X	X	X	X	X	X	X	X	X	X	X	X		
Penetration Test	H	H	H	H	E	H	H	H	E	H	E	E	H	E	E	H	E	E	E	E		
Oxidize Add'l 25 Hrs.	X	Xb	X		Xb	X	X	X					X	X	X	X						
Penetration Test	H	H	H		H	H	H	H					H	H	H	E						
Al <sub>2</sub> O <sub>3</sub> Sputter	X	X		X	X									X	X	X		X				
PT Sputter	X	X		X	X									X			X					
Pt-10RH Sputter	X	X		X	X									X			X					
Reoxidize, Age Hrs to 20 Megohms	X	X		X	X									X			X					
	25	75		75	25									25			25					
Measure Dielectric Breakdown	X	X		X	X		TO		50V						X			X				
Attach Leadwires	X	X		X	X									X			X					
20 Oven Cycles to 1250K	X	X		X	X									X			X					
Measure Insulation Resistance - Ambient to 1250K																				X		
Measure Thin Film Resistance	X	X		X	X									X			X					

Legend

X Completed

b Bluish Color

H and E are oxide hardness classifications. H indicates that the oxide was judged hard to penetrate E easy to penetrate, with a steel stylus of 0.64 mm tip diameter.

- |  |   |                                      |   |
|--|---|--------------------------------------|---|
| *1. MAR-M-509<br>(PWA 647)<br>Co - Based | 2. B1900 plus hafnium<br>(PWA 1455)<br>Ni - Based | 3. IN 100<br>(PWA 658)<br>Ni - Based | 4. MAR-M-200 plus hafnium<br>(PWA 1422)<br>(PWA 659 plus hafnium)<br>Ni - Based |
|--|---|--------------------------------------|---|

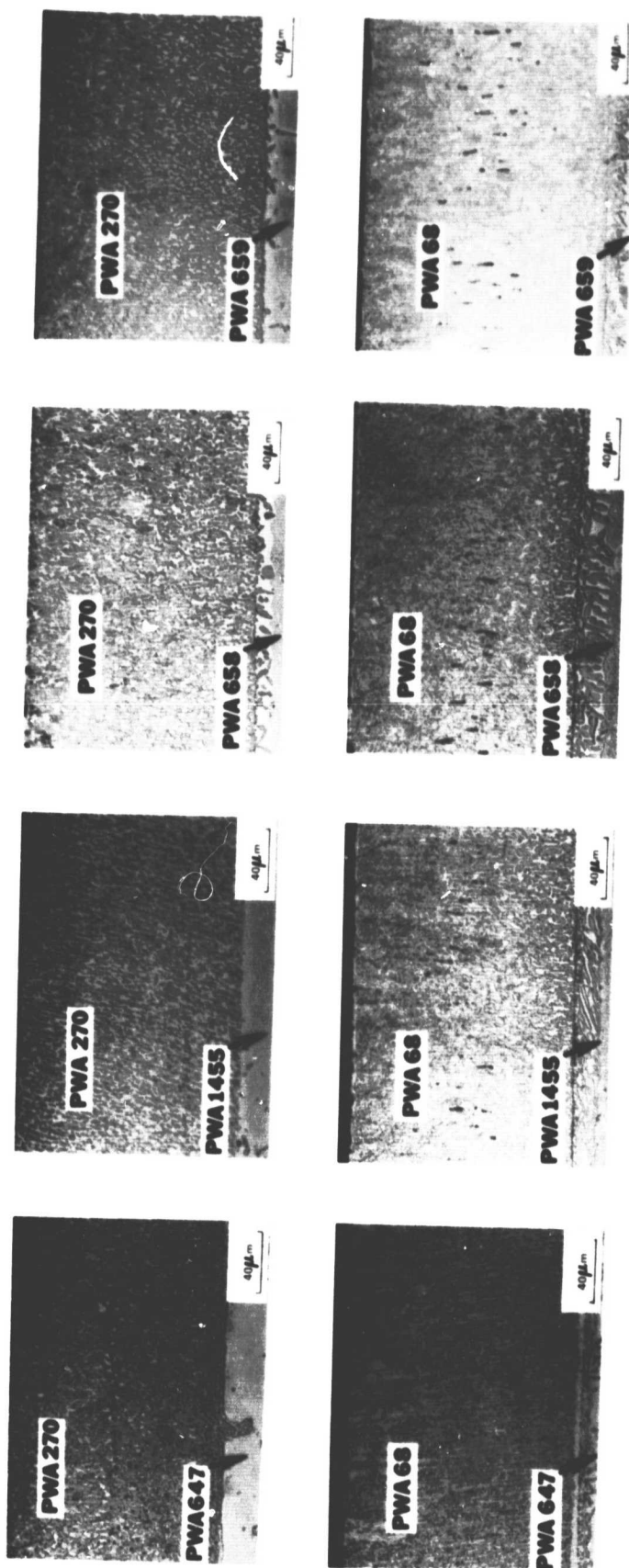


Figure 11 Morphology of NiCoCrAlY and CoCrAlY Coatings on Flat Plate Specimens of Four Turbine Blade Materials After Glass Bead Peening and Four Hours of Heat Treatment at 1340 K in Hydrogen Gas - The grain structure is excellent; a thin initial layer ( $\sim 1 \mu\text{m}$ ) aluminum oxide forms during the heat treatment, due to traces of oxygen in the hydrogen furnace.

ORIGINAL PAGE IS  
OF POOR QUALITY

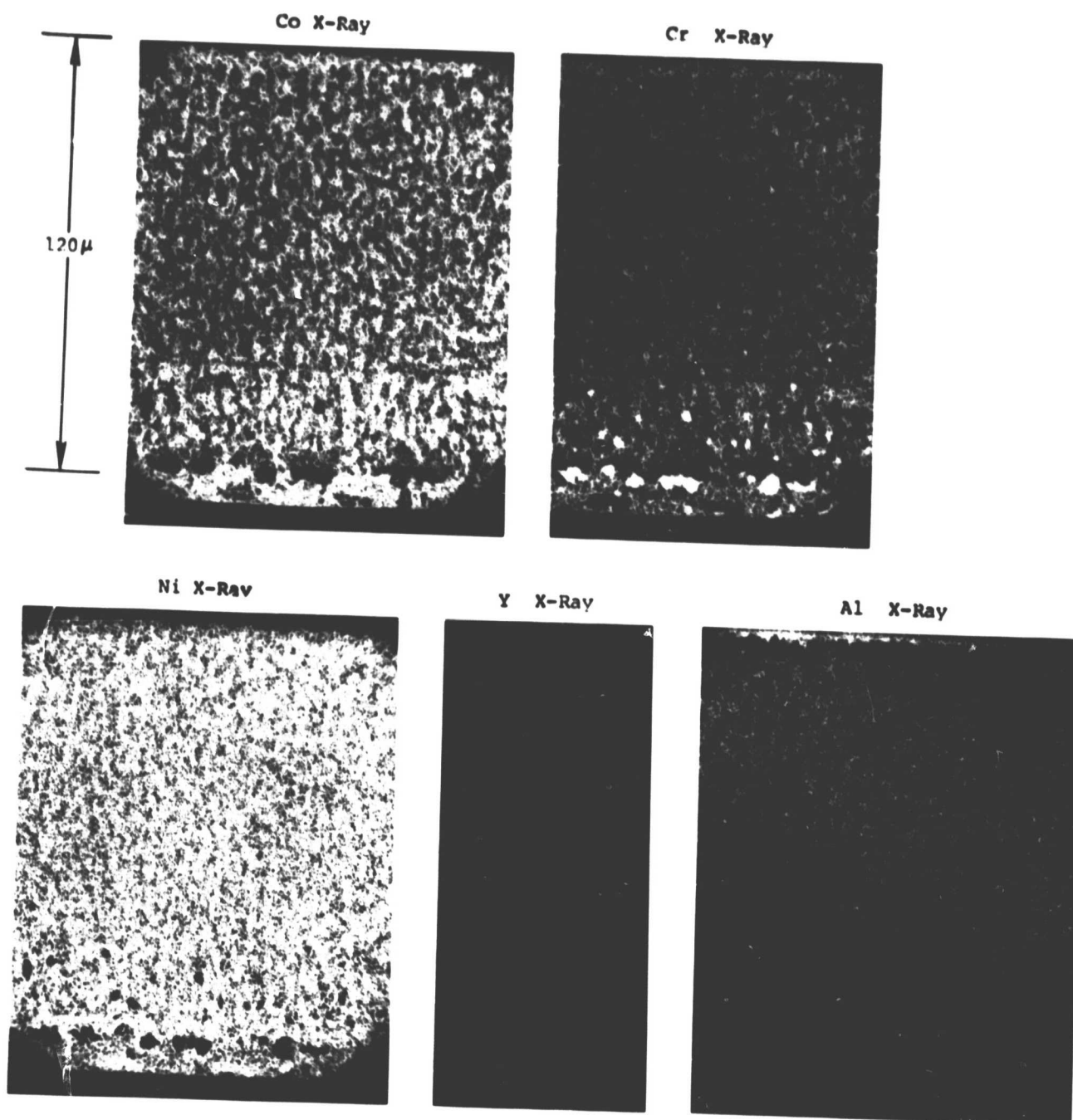


Figure 12 Chemical Composition Profiles of the NiCoCrAlY Coating on a MARM-200 + Hf Flat Plate Specimen After Four Hours of Heat Treatment in Hydrogen - Light areas denote higher concentrations. Aluminum is concentrated near the surface. An aluminum-depleted layer exists just below the surface.

OF POOR QUALITY

The appearance of bluish colors during heat treatment and oxidation on two specimens, signaling a possible excess of  $O_2$  (or other contaminants) during  $H_2$  heat treatment. The mechanical and electrical integrity of the oxide on these two specimens was not noticeably different from other specimens, however.

Eight selected pieces were sputtered with  $Al_2O_3$  and aged.

Six pieces were selected to include a sample of NiCoCrAlY on all four of the alloys and CoCrAlY on one Ni-based alloy and one Co-based alloy and thin films of platinum and platinum 10% rhodium were sputtered on them. Five of the test pieces were of the grooved type shown in Figure 3a, with the films sputtered in the pattern shown in Figure 3b, and one piece was of the hole type shown in Figure 3c, with films sputtered in the pattern shown in Figure 3d.

Electrical resistance between the sputtered platinum or platinum-10 rhodium thin films and ground immediately after sputtering varied from a few ohms for some stripes to above 20 megohms for others. The lower values were probably caused by local defects permitting penetration of the oxide structure by the high energy metal atoms during sputtering. It was found that 25 to 75 additional hours of oxidation at 1300K restored the insulation resistance to a value above 20 megohms for 77 percent of all thin films (65 out of 88), and for 91 percent of thin films on MAR-M-200 + Hf specimens (29 out of 32).

Dielectric breakdown voltage of the insulating layer was measured for the 65 films, that were 20 megohms above ground, by applying an increasing voltage until a current of 10 microamperes was recorded. The breakdown voltages fell between 5 volts and 50 volts, the lower values probably indicating local thin spots in the oxide. Since the average thickness of the oxide was determined to be about  $2 \times 10^{-4}$  from sample metallographic sections, the typical calculated dielectric breakdown strength was about  $10^5$  volts/cm, a value within the range reported by other investigators (Reference 10).

Leadwires were then attached to the films and the six specimens were temperature cycled in a furnace 20 times to 1250 K. Examination under an optical microscope at 200x showed no deterioration of the oxide or sputtered films. No change in insulation resistance at room temperature was observed. Tape tests showed a less than 1 percent loss of platinum or platinum-10 percent rhodium from the surface.

The effect of temperature on insulation resistance from room temperature to 1250 K was measured on Specimen No. 35, and the result is shown in Figure 13. The resistance decreased logarithmically from above 20 megohms at temperatures below 500 K to a few hundred ohms at 1250 K. This result is in agreement with published values.

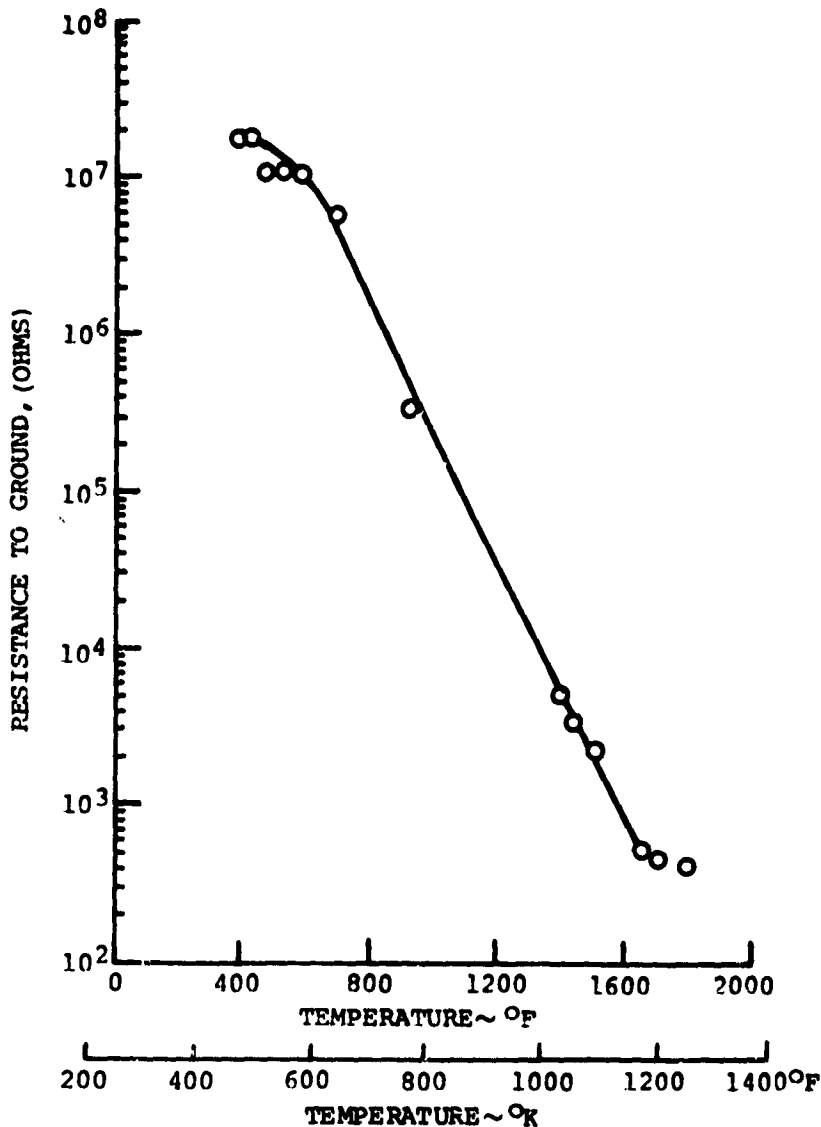


Figure 13 Measured Resistance to Ground for Platinum Thin Film - Sample 35.

The room temperature end-to-end resistance along the length of each platinum film was typically 1.7 ohms after sputtering and baking to achieve high resistance to ground. No important change occurred during the subsequent 20 cycles of furnace testing to 1250 K. The resistance of the platinum-10 percent rhodium lead films was typically 2.0 ohms after sputtering and baking and stable thereafter.

In summary, the two alumina forming coatings evaluated, CoCrAlY (PWA 68) and NiCoCrAlY (PWA 270), produced durable electrical insulation layers on four turbine blade and vane alloys evaluated at temperatures to 1250K.

On the most widely used turbine blade and vane alloy, the nickel based MAR-M-200 plus hafnium (PWA 1422), the NiCoCrAlY coating produced a hard initial alumina layer, while CoCrAlY produced a more easily penetrated initial alumina layer. On the other alloys (nickel-based B1900 plus hafnium (PWA 1455) nickel-based IN 100 (PWA 658), and cobalt-based MAR-M-509 (PWA 647), the two coatings both produced a hard initial alumina layer.

The fabrication of thin film sensor systems on a selected group of test specimens presented no compatibility problems. All sensors tested on all alloy-coating combinations passed the evaluation tests. MAR-M-200 + Hf coated with NiCoCrAlY was chosen for use in further testing because of its acceptable performance and its wide use.

#### 4.2 Thin Film-to-Lead Wire Connection

Ultrasonic welding was attempted. No bonding of platinum-10 percent rhodium was achieved. The manufacturers of the wire-to-thin film bonding machines commented that ultrasonic welding of the hard platinum-10 percent rhodium alloy was beyond the capability of existing equipment and that ultrasonic welding may be successful if higher wire to thin film forces were used.

Laser welding was also tried. In attempting fine wire to thin film welds, laser welding destroyed the thin film with no evidence of melting of the lead wire. It was suggested that if the laser beam diameter could be reduced to less than the wire diameter, success might be achieved. Samples of platinum-10 percent rhodium thin film on solid FeCrAlY substrates (which had been heat treated to form an insulating alumina layer) were sent to a vendor for trial. The wire was successfully attached to the surface but the thin films were electrically shorted to the substrate in the process. Additional heat treatment to 75 hrs. at 1300 K did not relieve the short. Visual examination of the surface in the area of the weld showed localized melting that apparently destroyed the insulation.

Although the bolted connection technique was successful, it was bulky and its practical application to engine parts such as blades or vanes would be difficult. The arrangement was a convenient one for furnace testing of thin film thermocouple systems on flat plate specimens.

The hot compression bonding technique, described in Section 3.2, was successful and was adopted for all lead wire bonding requirements in the program.

A series of experiments were performed using the hot compression bonding method. In the first successful platinum-10 percent rhodium bond experiments the assembly was placed in a clean oven and heated to 1140 K in air for 16 hours to form the bond. (Bonding could not be achieved at lower temperatures. The 304 stainless steel clamp material oxidized excessively at higher temperatures). The bond peel strength of several samples was measured by attaching a force gage to the free end of the lead wire and pulling the wire normal to the plane of the thin film. The average peel strengths were near 0.8 N. In most cases, the thin film to wire bond was stronger than the thin film to surface bond and bits of the thin film adhered to the wire during the peel tests. (The breaking strength of .075 mm platinum-10 percent rhodium wire is about 1.5 N.)

Electrical resistance measurements near the bonded area showed that the contact resistance was below 0.01 ohms.

Additional experiments showed that: Time at 1140 K required for bonding could be reduced to 4 hours with no noticeable decrease in bond strength; the strongest bonds occurred on clean as-sputtered films that were not previously heat treated or aged. If heat treatment is required prior to bonding, it must be done in vacuum or inert gas, to avoid formation of an oxide on the metal film surface.

The hot compression bonding process described above was also used successfully to bond two platinum-30 percent rhodium lead wires (.075 mm diameter) together, implying that the technique could be used in ANSI Type B thin film thermocouple systems.

#### 4.3 Thin Film Thermocouple Systems on Simulated Blades

##### 4.3.1 Overview

Table VI summarizes the simulated blade test results.

##### 4.3.2 Oven Calibration Tests

A record of a typical calibration cycle (simulated blade No. 4R<sub>1</sub>, 6/9/78) is shown in Figure 14, beginning with a 4-hour warmup to 1250K, then the 2-hour soak at 1250K, and ending with a 3-hour cool down to room temperature. Figure 15 shows the temperature profile on the simulated blade at two different times in the calibration cycle, one during the steady-state soak and the other during the cooldown period.



TABLE VI

## TEST RESULTS: SIMULATED TURBINE BLADES

Specimen No.	First Group			Second Group			Supplementary Group		
	4L <sub>1</sub>	4R <sub>1</sub>	2R <sub>1</sub>	3R <sub>1</sub>	2L <sub>1</sub>	3L <sub>1</sub>	6L <sub>2</sub>	2R <sub>2</sub>	6R <sub>1</sub> 4L <sub>2</sub> 6L <sub>2</sub>
Oven Test									
1 Error, TFT No. 7, %	1.8	1.1	2.9	2.0				3.5	4.08
2 Error, TFT No. 6, %	1.0	1.0	1.2	1.9				0.5	N.A.
High Temperature									
Exhaust Gas Flow Test									
1 Error, TFT No. 7, %	1.8	0.0	N.A.	N.A.	2.4	0.9	1.6	3.5	N.A.
2 Error, TFT No. 6, %	0.0	0.0	3.9	N.A.	3.6	1.7	-1.4	-1.4	N.A.
3 Hrs. to Fail No. 7	0.156	0.906	0.016	.006	585	476	547	497	509
3 Hrs to Fail No. 6	0.156	0.506	0.406	.006	585	246	147	337	N.A.
4 Survival Factor	0.01	0.02	0.01	0.00	1.00	0.61	0.59	0.71	N.A.
Av. Survival			0.01			0.73			N.A.
Delivery to NASA					X				X X

## Notes

1. Error =  $100 (T_3 - T_2) / 1250$ ; All Temperatures K
2. Error =  $100 (T_2 - T_6) / 1140$ ; All Temperatures K
3. Failure is Defined as Drift More Than 4% or Open or Short
4. Survival Factor is Failure Time (Hrs.) Divided By 58
5. No Failure
6. Platinum Thin Film Separation
7. Platinum - 10% Rhodium Thin Film Open
8. Chromium Precoated Platinum Thin Film
9. Endurance Test of Platinum Thin Film, 50 Hrs. 10 Cycles

N.A. = Not Applicable

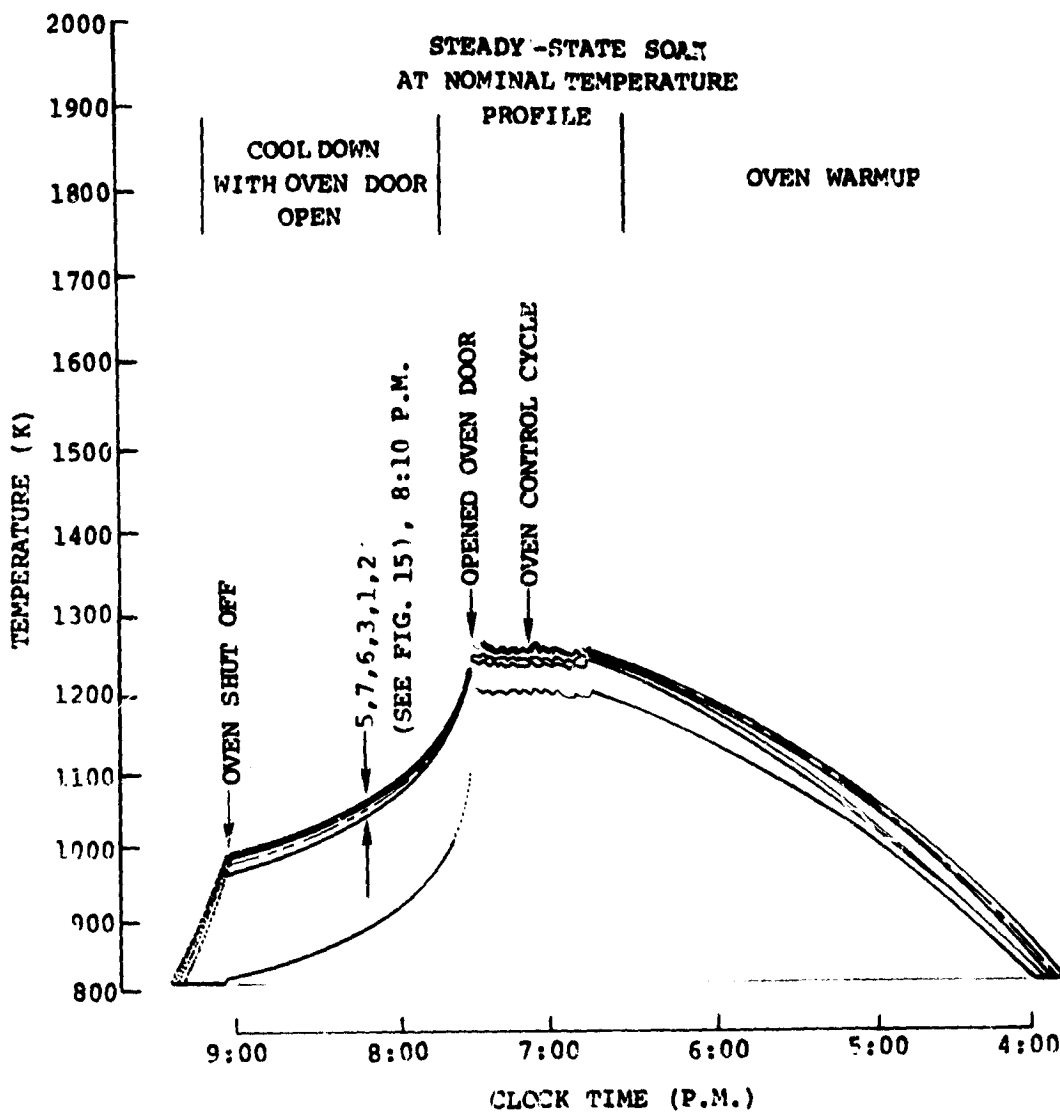


Figure 14 Chart Recorder Trace of Indicated Temperature versus Time During Oven Cycle of Simulated Blade 4R<sub>1</sub>

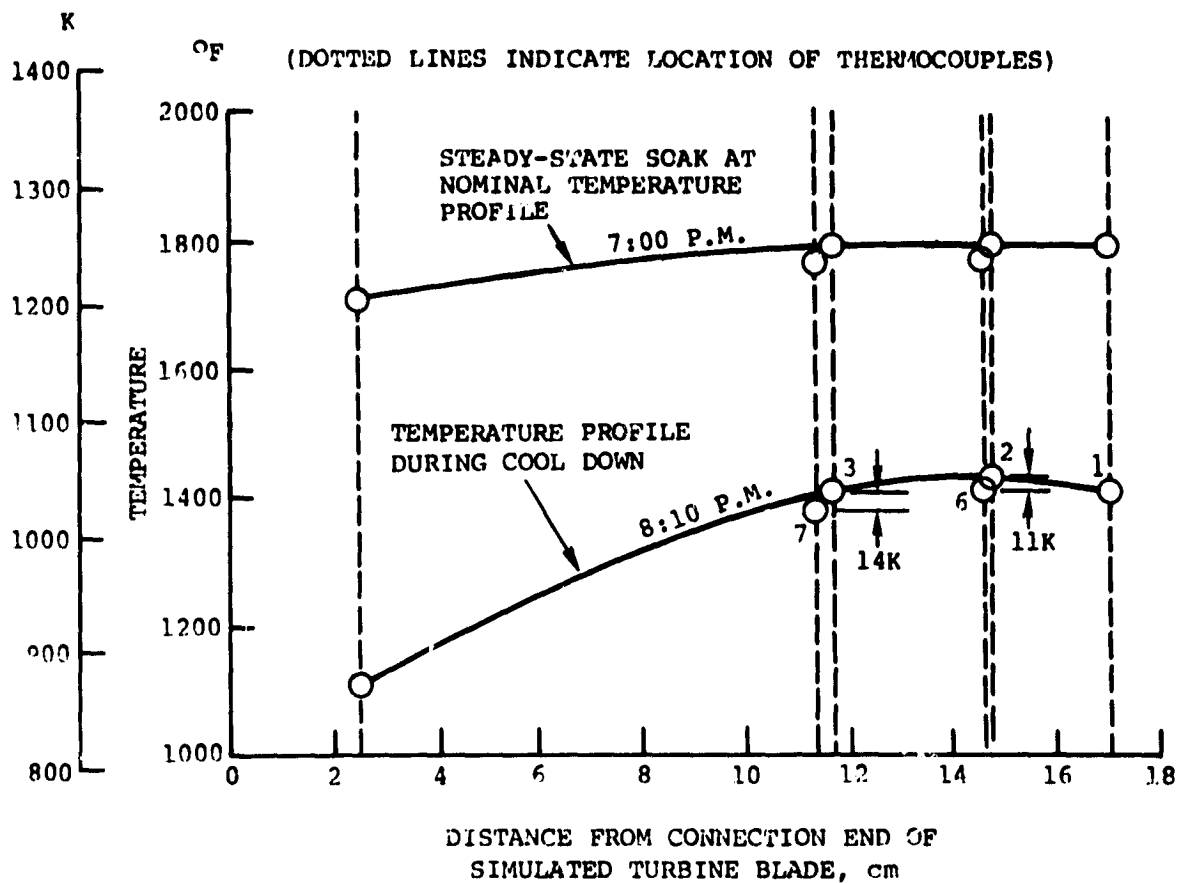


Figure 15 Indicated Temperature versus Distance from Lead Wire End of Simulated Turbine Blade at Two Different Times During Oven Test - Dotted lines indicate the location of thermocouples.

Note, in Figure 14, that each thin film thermocouple reads slightly lower (1 percent to 2 percent) than its adjacent reference wire thermocouple. For the ten thermocouple systems that were calibrated in oven tests, Table VI shows that the thin film thermocouples read from 0.5 to 3.5 percent lower than the adjacent reference thermocouple. The average was 1.7 percent and the standard deviation 0.8 percent. The offset was about the same during the 1250 K soak, when the temperature gradient along the specimen was about 55 K as it was during the cooldown when the temperature gradient was about 160 K. The offset in the sputtered thermocouple system is ascribed to a slight departure from the standard Type S calibration curve. A 10K to 25°F offset would occur if the rhodium content of the platinum-10 percent rhodium leg were 9.5 percent rather than 10 percent, for example. Electron microprobe analysis of the thin film surface on a sample specimen indicated that the rhodium content was between 9 percent and 11 percent. The uncertainty in this measurement was thus too large to verify whether the offset was due to low rhodium content.

The calibration of each individual thin film thermocouple was stable within 0.5 percent throughout its oven calibration cycle. The differences in calibration between thin film thermocouples are therefore significant. It would appear that at this stage of development each thin film thermocouple requires individual calibration to obtain the objective of 1.2 percent accuracy.

#### 4.3.3 Vibration Tests

Simulated Blade No. 4L<sub>1</sub> was vibration tested prior to hot gas flow testing, and No. 4R<sub>1</sub> was vibration tested after hot gas flow testing. The test procedure, involving 1 hour of shake testing on each of three axes, is described in Section 3.5.

Post-test examination showed no deterioration of any kind. The lead wire to thin film connections and thin film to alumina bonds remained mechanically sound. There was no change in electrical resistance to ground or in electrical continuity in the two thin film thermocouple systems. The error in indicated temperature of the two systems on 4L<sub>1</sub>, during subsequent testing in the 1250 K combustor flow, were both within 1.1 percent of the values determined in oven calibrations conducted before the vibration tests.

The negligible effect of vibration on sputtered thin films was to be expected, since the mechanical stresses involved are orders of magnitude smaller than the stresses arising from thermal gradients in oven tests and in the hot gas flow environment. The vibration tests were most important in establishing the durability of the thin film-to-leadwire connections.

#### 4.3.4 High Temperature Exhaust Gas

After oven testing, each of the first four simulated blades was installed in the exhaust stream of a test combustor for 1250 K hot gas flow testing. The desired temperature profile (Figure 9) was established by adjusting the combustor nozzle size and specimen location.

On two of these simulated blades ( $2R_1$  and  $3R_1$ ), the four thin film thermocouple systems either open circuited or became erratic immediately so that no useful temperature indications were obtained. On the other two simulated blades ( $4L_1$  and  $4R_1$ ), the systems provided stable temperature readings, for periods of 10 minutes to 55 minutes before open-circuiting. For each thin film thermocouple on each of these two specimens the indicated temperature error was within 1.1 percent of that observed during the oven calibration, showing that the cooldown at the end of oven tests, reheat at the start of combustor tests, and vibration testing of  $4L_1$  (described in Section 4.3.3) had no serious effect on the calibration of the thin film thermocouple.

Examination of the four specimens showed that all eight thin film thermocouple failures were caused by separation of the platinum films at the center (hottest part) of the specimens. Platinum-10 percent rhodium adherence was generally excellent. One platinum-10 percent rhodium film showed slight indications of deterioration after 55 minutes. Thin film-to-lead wire connections were unaffected by the combustor testing.

The platinum adherence problem was believed to be associated with surface contamination of the specimens at either the oxidizing or sputtering stage of fabrication. Surface contamination (particularly moisture) is known to affect the adherence of platinum films much more than the adherence of platinum-10 percent rhodium films.  $Al_2O_3$ , tape adhesives and photoresists are all hygroscopic, and humidity in the laboratory was unusually high (above 60 percent) at times during fabrication. Prolonged initial sputter etching of photoresist-masked specimens was found to result in a poorer adhesion of platinum, probably because of transfer of photoresist material to the clean unmasked area. Use of a negative photoresist, permitting tape to be applied on top of a photoresist layer and avoid contact of tape to alumina, was not found advantageous. Removal of the negative photoresist residue was more difficult than removal of the tape residue.

After these investigations were completed, a second set of six simulated blades was fully instrumented. Four of these were subjected to a 57.7 hour 1250 K hot gas test. The tests were conducted in the hot flow stream of the oxyacetylene torch (Figure 10). The time history of each test is shown in Figure 16 and the results are summarized in Table VI, Columns 5 through 8. In Figure 16 each point plotted is the average of 10 to 30 readings obtained during the constant temperature portion of one cycle. Standard deviation of all points in one cycle rarely exceeded 1 percent. An omitted point represents a case where flame control was erratic and reliable reference wire thermocouple readings could not be obtained.

The survival factor is defined as the percentage of overall test time that each thin film thermocouple remained operative, while output remained within 4 percent of the output of the adjacent reference wire thermocouple. The average survival factor for the 8 thermocouples was .73 (or 42 hours out of 58 hours of total test time). Two thermocouples on test specimen 2L<sub>1</sub> survived the entire test. (survival factor = 1.0)

Figure 17 is a plot of the change in error, or drift, with time of the eight thin film thermocouples. The drift has been normalized to a value of zero at a starting time of near zero. The drift in indicated temperature is generally downward at a rate of less than 0.1 percent per hour. In only two cases did the cumulative drift exceed  $\pm 1$  percent during the first ten hours. In no case did the cumulative drift exceed 2 percent during the first 20 hours or 4 percent during the first 50 hours.

Resistance to ground was generally above  $10^7$  ohms at room temperature and above  $10^4$  ohms at 1250 K. A notable exception was the unusual behavior of thin film thermocouple 7 on specimen 6L<sub>2</sub>, (Figure 16C). This thermocouple had only a few ohms resistance to ground at one thin film-to-lead wire connection initially, apparently due to excessive force during hot compression bonding. The thermocouple system nevertheless performed well for 54 hours and 16 temperature cycles (Figure 16C) failing finally by open circuit near the center (hottest part) of the specimen. The testing was continued, and at 57 hours, (23 cycles), it began functioning again, but now it was indicating the temperature of the lead wire end of the bar. It was found that both thin film-to-lead wire connections were now grounded at this point, forming an effective thermocouple junction there. This experience emphasizes the advisability of checking resistance-to-ground from time to time, since in an actual engine test, low resistance-to-ground could signal the formation of a new thermocouple junction.

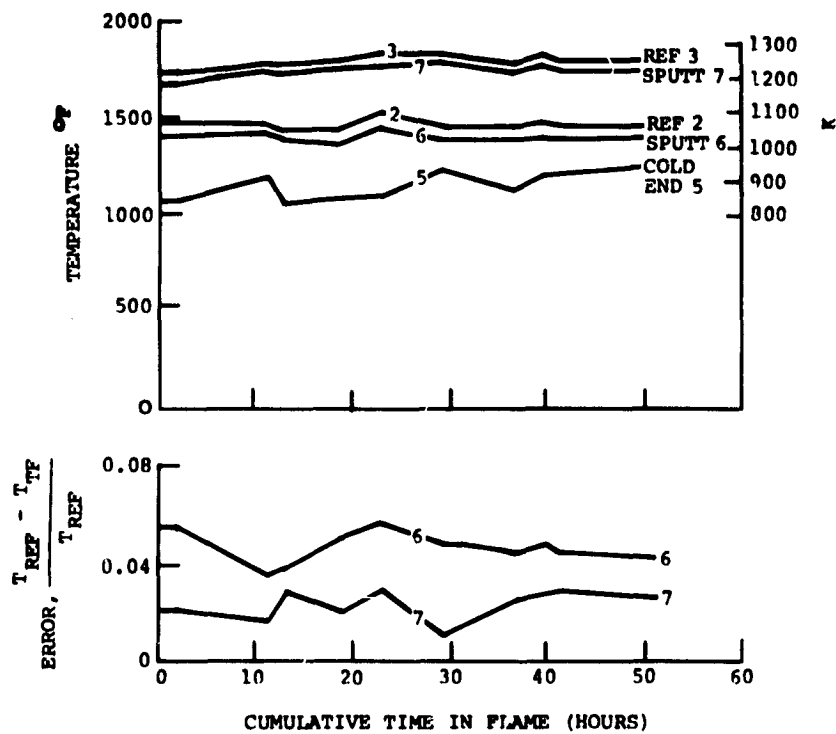


Figure 16a Indicated Temperature versus Time During Simulated Turbine Blade Exhaust Gas Flow Tests, Simulated Blade 2L<sub>1</sub>

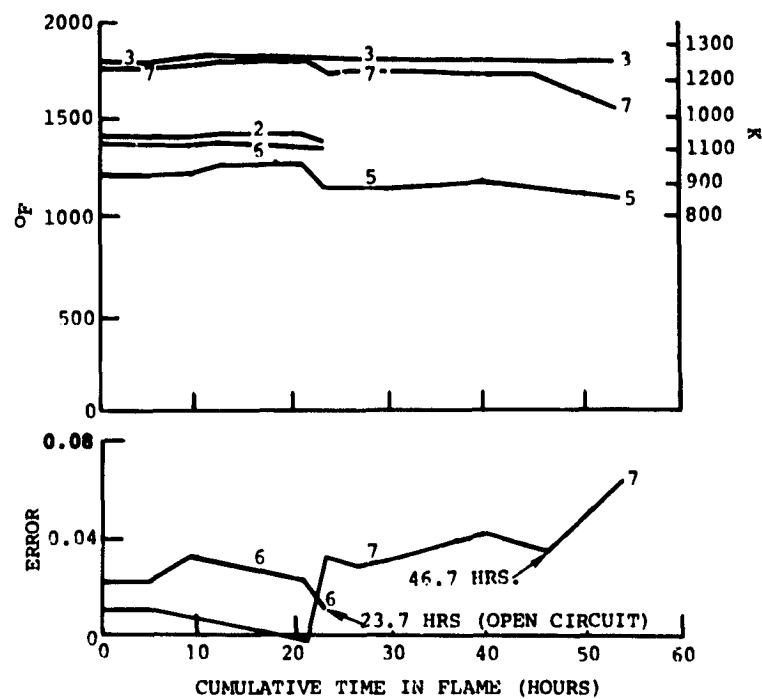


Figure 16b Indicated Temperature versus Time During 1250 K Gas Flow Cycling Tests, Simulated Blade 3L<sub>1</sub>

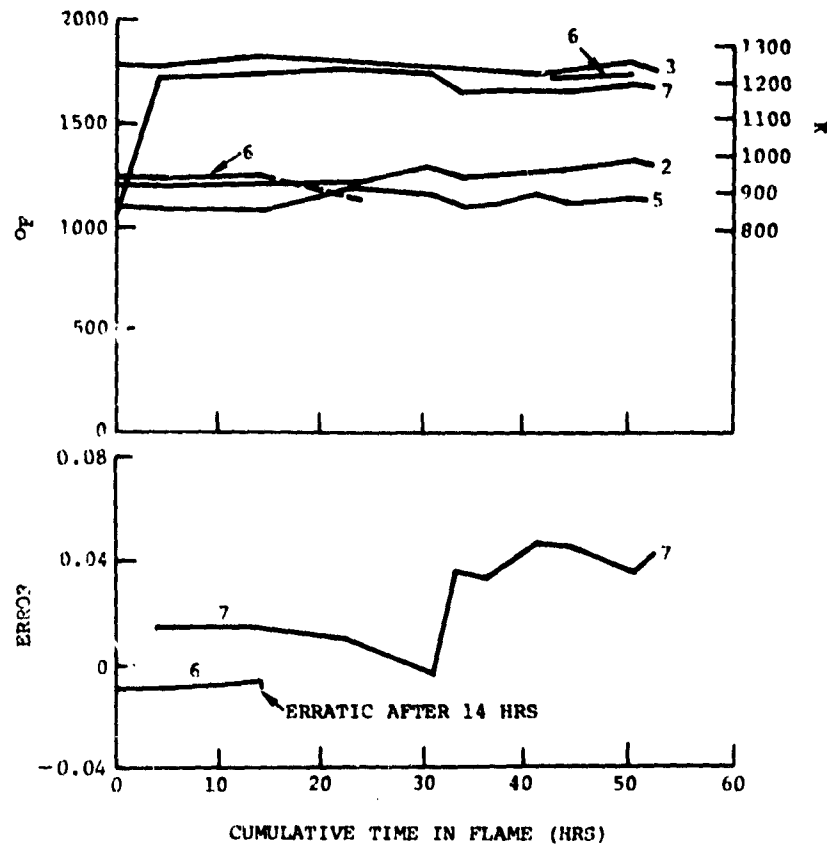


Figure 16c Indicated Temperature versus Time During 1250 K Gas Flow Cycling Tests, Simulated Blade 6L<sub>2</sub>

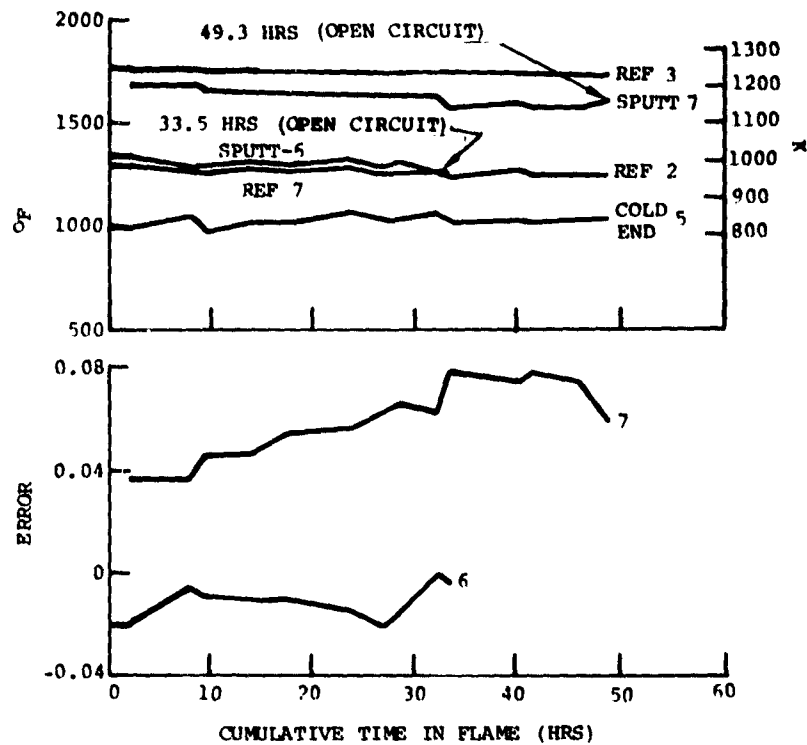


Figure 16d Indicated Temperature versus Time During 1250 K Gas Flow Cycling Tests, Simulated Blade 2R<sub>2</sub>



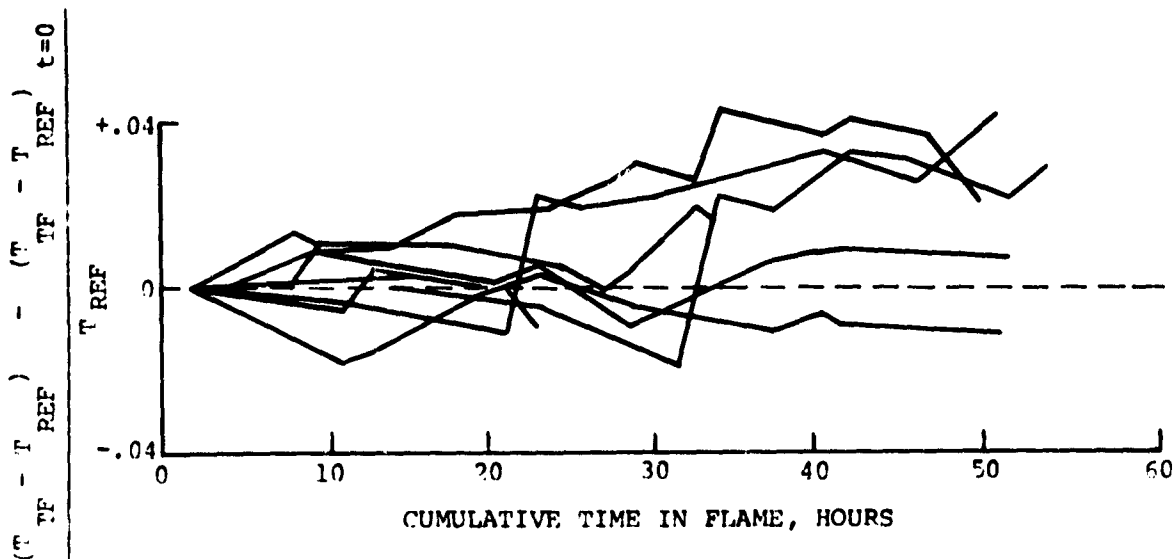


Figure 17 Relative Drift in Calibration of Eight Thin Film Temperature Sensor Systems on Simulated Blades During 1250 K Exhaust Gas Flow Tests ( $T_{TF}$  is thin film thermocouple temperature and  $T_{REF}$  is the adjacent reference wire thermocouple temperature)

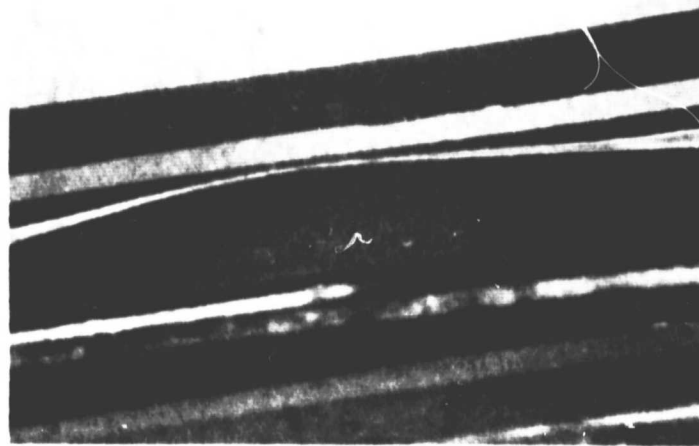
Post-test examination of the specimens revealed that where failure occurred, the failure was one of the two following types:

- a) Separation or lifting of the platinum film lead from the oxide surface, eventually leading to an open circuit in the platinum lead when a section of the unsupported platinum film disappeared completely (Figure 18A).
- b) Development of one or more hairline cracks of the oxide surface, leading to an open circuit in the hard, adherent platinum-10 percent rhodium lead film (Figure 18B).

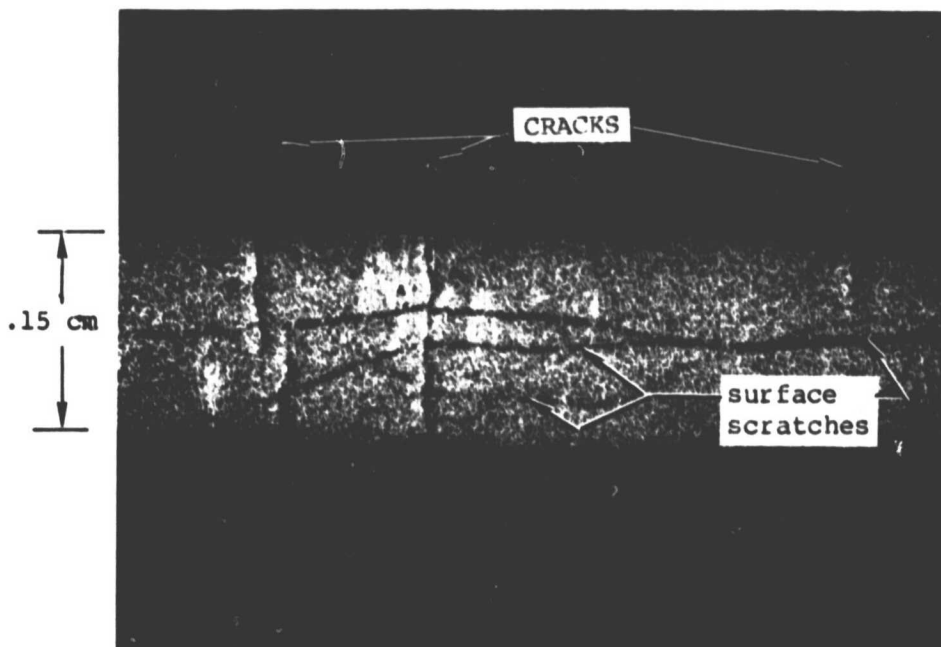
Both types of failure occurred only in the center portion of the simulated blade where the temperature was between 1150 K and 1250 K. No mechanical failure of the lead wire attachments occurred.

Failure of platinum adhesion was by far the predominant failure mode with 10 failures. Local cracking of the oxide occurred on two specimens, both of which had been reworked several times and were subjected to many more temperature cycles than the other simulated blades. Additionally, the poor adhesion of platinum films did not appear to originate at cracks in the oxide, whereas failure of platinum-10 percent rhodium films occurred only at cracks in the oxide.

Although the minimum goals of 75 percent survival factor were achieved with the final group of test pieces, the platinum adhesion problem was severe enough to warrant further study. Therefore, after a literature search and discussions with consultants, approaches to further improve platinum adhesion were identified.



(A) Peeling of Platinum Film During Torch Flame Testing of Simulated Blade. Blade No. 2R<sub>1</sub> TC No. 6. Film width is .15 cm.



(B) Cracking of Platinum -10% Rhodium Film Due to Cracking of Aluminum Oxide Layer During Torch Flame Test of Reworked Simulated Blade. Blade No. 6L<sub>2</sub> TC No. 7.

Figure 18 Thin Film Temperature Sensor Failure Modes

## 5.0 THE PLATINUM ADHERENCE PROBLEM

### 5.1 Overview

In this section the results of a brief theoretical and experimental investigation of the mechanism of adherence of thin metal films to other materials are presented. In the case of adherence of platinum to alumina, three promising techniques worthy of further evaluation are identified: field assisted bond, reactive sputtering, and sputtering of an interlayer of a metal other than platinum between the platinum film and the alumina.

### 5.2 Principles of Metal Film Adherence

Adherence is partly electrical and partly mechanical in nature. Electrical contributions to adherence, discussed lucidly by Masterton and Slowinski in Reference 24, include all the chemical atom-to-atom bond mechanisms (ionic, covalent, non-polar, metallic) and all the chemical molecule-to molecule bond mechanisms (dipole forces, hydrogen bonds, and the dispersion or London forces). The mechanical contributions include pegging, embedment, reticulation (interweaving of fibrous materials), and reentry topology, which may exist on any scale from the atomic up to the readily visible.

The conditions at the interface are usually quite complicated electrically because of the presence of several atomic species of different atomic radius and electron configurations - some species arranged in the form of well defined stable molecules, some in the form of a regular metallic lattice, and some (contaminants) poorly defined or unknown. The conditions are complicated mechanically as the result of previous mechanical polishing or roughening, the presence of intersecting grain boundaries, whiskery or hairy structures, and embedded foreign objects.

The electrical cohesion of a metal to itself or to another metal is quite different in principle from the electrical cohesion of a molecular ceramic (such as alumina) to itself or to another ceramic.

Cohesion within a metal is due to the electrical metallic bond. The positively charged atomic nuclei are arranged in a regular lattice (within each metal grain) and the intervening spaces may crudely be thought of as filled with a sea of negatively charged electrons. Some of the electrons are mobile and may move through the lattice, but at any instant the array of stationary positive nuclei and mobile negative electrons results in a balance between electric repulsion forces (positive repelling positive and negative repelling negative) and electrostatic binding forces (positive attracting negative) that hold the material in equilibrium. The forces are weaker across grain boundaries, where the lattice abruptly changes direction. If two pieces of the same metal are pressed firmly together at an atomically clean

interface (no foreign matter) with force enough to bring the lattices into close contact - i.e., an interface region no thicker than a grain boundary - then the two pieces after some time will become one. This is the principle of hot compression bonding.

If two different metal species are pressed together, a strong bond may or may not form. It appears that the best adhesion occurs if the two metals have nearly equal atomic radii, within +5 percent, and nearly equal electronegativity (affinity for electrons) within +5 percent. (References 11, 22) In this case the two metals will exhibit a wide range of solid solutions (Reference 22) so that atoms of one may readily substitute for atoms of the other in either lattice structure. Poorer adhesion results if these conditions are not met, or if intermetallic chemical compounds form at the interface (usually brittle; see References 15, 17, 19). Note that free diffusion of one metal into another does not assure permanent adhesion; Reference 13 provides a good example of excellent bonding (Au to Ta) without extensive diffusion, and there are many pairs of metals in which mutual diffusion occurs readily but bonding is poor because of incompatibilities in atomic radius or electronegativity or because brittle compounds form. Diffusion tends to proceed first along grain boundaries, providing mechanical pegging between two species. Diffusion within the lattice, and formation of intermetallic compounds (if any) occurs later. All of these processes are accelerated at higher temperatures, and the grain size itself usually grows larger with time at elevated temperature, reducing adherence.

Cohesion within a molecular non-conductor (e.g.,  $\text{Al}_2\text{O}_3$ ) is due partly to static dipole forces and partly to the so called dispersive or London forces which are temporary, dynamic dipole forces. The electrons are firmly bound within each molecule and do not move through the material. Dipole forces arise if the molecule is electrically assymetric. One end of each molecule then has a slight positive charge and the other end a slight negative charge (dipole). The molecules tend to line up, positive attracting negative, forming a stable structure. The dispersive forces have the same nature but occur even when the molecule is symmetric. Because of the continuous motion of electrons within each molecule, at any instant a particular symmetric molecule may temporarily exhibit a positive charge at one end. This tends to cause the adjacent molecule to temporarily form a negative pole at the adjacent end. While on the average there is no dipole structure, at any instant there are strong electrical forces binding one molecule to the next.

If a piece of  $\text{Al}_2\text{O}_3$  is pressed against a piece of metal at an atomically clean interface, it is not immediately clear that any strong electrical cohesive force should arise, since the structures are radically different. In fact it is found that cohesion can be quite strong (References 11, 12, 14, 23), if the metal is one that oxidizes readily. It therefore appears that an electrical mechanism is at work,

probably ionic bonding of metal nuclei (ions) to oxygen ions in the  $\text{Al}_2\text{O}_3$  at the interface, perhaps again on a statistically time varying basis. Mechanical bonding will occur, if the surface is atomically rough and defective, providing sites for embedment, and if the mechanical interface is characterized by short wave length jaggedness, providing large surface area of contact per unit of plan view surface area. Small grain size in the metal (characteristic of thin films) may be advantageous, providing a large number of grain boundaries where interpenetration can occur readily. In some special cases the metal (X) and the  $\text{Al}_2\text{O}_3$  can combine chemically to form  $\text{XAl}_2\text{O}_4$ , a spinel, providing enhanced adhesion (Reference 19). This reaction seems to account for the strong adhesion to  $\text{Al}_2\text{O}_3$  of some metallic inks used in printed circuits (Reference 23).

If a voltage gradient is applied across the metal (+) to a nonconductor (-) interface while heating to a temperature at which the nonconductor becomes slightly conductive, then adherence is greatly enhanced. This process, often called field assisted bonding, is described in a U.S. Patent by Pomerantz (Reference 12) and data is provided showing a tenfold improvement in adherence of Au, Mo, and Al on glass. The reference also states that the process is appropriate for platinum on alumina, though no data is provided for this case. The electrical mechanism at the interface is not described; some combination of migration and electrostatic polarization presumably occurs.

### 5.3 Approaches to Improving Adherence of Platinum on Alumina

Since platinum does not readily oxidize and forms no known spinel with alumina, adherence of pure platinum on pure alumina in the absence of an imposed electric field is presumably mainly mechanical. The fabrication procedure outlined in Table IV promotes mechanical adherence in several ways:

The controlled surface finish, with polishing followed by grit blasting, has been determined to be an excellent surface for metal-to-oxide bonding. (ref. 5).

The cleaning procedures are designed to keep the surface free of contaminants.

Radio-frequency sputtering is a film-deposition process which is recommended for its good adherence characteristics.

Despite these considerations, the resulting platinum film is not as adherent as platinum-10 percent rhodium films fabricated using the same technique. The presence of rhodium, which oxidizes much more readily than platinum, apparently provides additional electrical (ionic) bonding in the platinum-10 percent rhodium leg.

The four following approaches to improving the adherence of thin film thermocouple systems are suggested by the previous analysis.

1. Change from sputtered Type S thermocouples (platinum vs platinum-10 percent rhodium) to sputtered Type B (platinum-6 percent rhodium vs platinum-30 percent rhodium) to eliminate the platinum leg. The objections are that platinum-6 percent rhodium may still be less adherent than platinum-10 percent rhodium, that platinum-30 percent rhodium is extremely hard and brittle and may raise new durability problems (through it was found that platinum-30 percent rhodium lead wires could be hot compression bonded reliably), that Type B thermal emf is too small for accuracy below 1100 K and that the cost of fabrication would be increased since two expensive binary alloys would require control rather than one.
2. Apply field assisted bonding. After sputtering platinum on alumina, apply a d.c. voltage between the platinum film (+) and the base material (-), while heating to a temperature at which the alumina is slightly conductive. Reference. 12 provides details.
3. Vary sputtering parameters to enhance adherence characteristics. Substrate temperature, bias, process energy, spacing, pressure, and sputtering rate can all have an effect on the adherence of the deposited film. An experimental program to determine optimum parameters could be undertaken.
4. Reactively sputter the platinum lead film, to promote adherence by promoting the formation of oxides which do not readily form otherwise. In reactive sputtering the ionized gas mixture used in the sputtering process contains an atomic species (typically oxygen) which can react with the thin film or with the substrate. Initial reactive sputtering with oxygen followed by normal sputtering with argon has been used to improve the adherence of gold (Reference 11) and to produce thin films of platinum monoxide (Reference 25). Platinum monoxide is volatile at temperatures above about 700 K, but be stable if deposited as a layer a few dozen nm thick beneath the 2.0  $\mu$ m layer of platinum.
5. Sputter an interlayer of a second metal or alloy between the platinum and the alumina. The metallic layer must bond well to both, be stable at high temperature, and not introduce a strong new thermal emf or drift in calibration in the system. This new metal must oxidize more readily than platinum (in order to bond to the alumina) and must also form a wide range of solid solutions with platinum (in order to bond to the platinum). Logical candidates are rhodium, platinum-10 percent rhodium, and chromium. Several successful systems of this kind are reported in the literature, including molybdenum between gold and cadmium sulphide (Reference. 16), molybdenum on vanadium (Ref. 18), and platinum on chromium (Reference 20).

Experiments with each of the last three techniques were carried out during the present program, with the following results:

Variation in Sputtering Parameters: The sputtering parameters used in the program for sputtering of thin films of platinum on masked substrates were established by experience. Variations of the parameters to promote the adhesion of platinum films are necessary restricted because of the temperature limitation of 440K imposed by the organic masking materials. These materials decompose at higher temperatures of operation and contaminate unmasked areas, resulting in reduced adherence of sputtered films.

Both sputter etching and bias sputtering were tried for brief periods with no observable change in the adhesion of platinum. Higher energy levels and substrate cooling are probably required to achieve significant improvement through adjustment of sputtering parameters.

Reactive Sputtering: Three platinum lead films were sputtered on one of the preliminary flat plate specimens, Section 3.1, using 50 percent oxygen, 50 percent argon for 5 minutes and 100 percent argon for the balance of the one hour sputtering run. The piece was then cycled ten times to 1250 K and held for one hour at 1250 K in each cycle. Subsequent vigorous tape testing failed to remove any platinum.

Chromium Precoat: One 2.0  $\mu$ m platinum lead film of thermocouple No. 7 on simulated blade No. 6L<sub>2</sub> (Figure 7) was sputtered over an 80 nm film of chromium. The simulated blade was subjected to the oven calibration procedure, Section 3.4, and the 50 hour, ten cycle, 1250 K exhaust gas flow test, Section 3.6, plus one four hour exhaust gas test at 1366 K. There was no visible deterioration of the platinum lead film. After all testing was completed, repeated vigorous tape testing finally resulted in some separation of the platinum from the chromium. The adherence was judged excellent. During the oven test, there was a gradual drift in thin film thermocouple calibration (four hour soak at 1250 K). The error was 2.2 percent at the start and 5.0 percent at the finish. The temperature gradient along the simulated blade was increased after one hour from 80 K to 160 K by opening the oven door. There was no noticeable change in thin film thermocouple reading associated with this change in the gradient. The drift in calibration is attributed to a gradual change in composition of the platinum leg due to diffusion of chromium. It is expected that a thinner chromium precoat and further aging would reduce this effect to less than 0.1 percent per hour from the present 0.7 percent per hour. Thin film thermocouple readings were not recorded during the exhaust gas testing.

Platinum-10 Percent Rhodium Precoat: One 2.0  $\mu$ m platinum film (fabricated using the procedure described in section 3.1 on JT10D-2 turbine blade No. 1 under Contract NAS3-20831) was sputtered over a 5.0  $\mu$ m film of platinum-10 percent rhodium. A Type S thin film thermocouple without precoat was fabricated on the same blade. No lead



wires were attached since this was a preliminary blade specimen intended for film durability testing on an actual turbine blade. The blade was then oven cycled ten times to 1250 K and held for one hour at 1250 K in each cycle. Subsequent vigorous tape testing failed to remove any of the thin films. While this result did not prove the superiority of precoating with platinum-10 percent rhodium, since all films survived, it does encourage further testing.

The results of the literature review and experimental evaluations suggest that a significant improvement in adhesion of platinum to alumina is probably achievable. Testing of statistically significant numbers of samples is recommended.

## 6.0 CONCLUDING REMARKS

A detailed procedure was developed for fabrication of thin film thermocouple systems on turbine blades, for the purpose of measuring metal surface temperatures in operating engines. The procedure uses alumina-forming MCrAlY coating technology to produce alumina insulating layers, radio frequency sputtering of platinum and platinum-10 percent rhodium to produce thin film thermocouples, and hot compression bonding to attach lead wires.

The two alumina forming coatings evaluated, CoCrAlY (PWA 68) and NiCoCrAlY (PWA 270), produced durable electrical insulation layers on four turbine blade alloys evaluated at temperatures to 1250K.

On the most widely used turbine blade alloy, the nickel based MAR-M-200 plus hafnium (PWA 1422) the NiCoCrAlY coating produced a hard initial alumina layer, while CoCrAlY produced a more easily penetrated initial alumina layer. On the other blade alloys (nickel-based B1900 plus hafnium (PWA 1455), nickel-based IN 100 (PWA 1455), nickel based IN 100 (PWA 658), and cobalt-based MAR M 509 (PWA 647), both coatings produced hard initial alumina layers.

The fabrication of thin film thermocouple systems of Pt/Pt10Rh on test pieces made from various alloy-coating combinations showed no compatibility problems. MAR-M-200+Hf coated with NiCoCrAlY was chosen for use in subsequent testing because of its acceptable performance and wide use.

Hot compression bonding of lead wires to thin films (platinum to platinum and platinum-10 percent rhodium to platinum-10 percent rhodium) was shown to be reliable and repeatable using the technique developed in this program. There were no failures in the 32 connections used in extensive testing under simulated engine turbine conditions.

Four simulated turbine blades were fabricated, each containing two thin film thermocouple systems, and subjected to an exhaust gas flow at 1250K. These tests were hampered by adherence failures of the platinum thin film.

Following an analysis of the adherence problem, four more simulated turbine blades were fabricated, also with two sensor systems each. These test pieces were subjected to a test program consisting of a total of 58 hours at 1250K in an exhaust of an oxyacetylene flame, 31 thermal cycles from ambient to test temperature, and various calibration tests.

The average life of the eight systems was 42 hours at 1250K, where failure is defined as either an open circuit or a four percent shift in calibration (percentage error based on absolute temperature).

The survival factor for these sensor systems, defined as average life/total test time, was about 0.75, which was the goal of the test program.

Standard deviation in the life of the present sensor systems is 0.37.

The primary failure mode is an open circuit in the platinum film in the hottest region of the surface of the simulated blades, resulting from poor adherence and peeling of platinum in this region, just as in the first group.

Two sample systems of the eight systems tested completed 57.7 hours at 1250 K without failure, and without any detectable peeling of platinum films.

A secondary failure mode was cracking of the alumina insulating layer in the hottest region of the Pt-10 Rh films (two failures).

Vibration testing for 1 hour at 8 g peak, 100 to 400Hz, on each of three axes, before or after temperature cycling to 1250 K had no detectable effect on durability or calibration error of the sensor systems.

The thermal emf of the systems was independent of temperature gradients along the films within the  $\pm 1$  percent accuracy of the experiments for temperature gradients of 50 K to 220 K.

The initial thermal emf (at the start of 1250 K gas flow cycling tests) of the thin film thermocouple systems varied significantly from sample to sample, with equivalent temperature errors relative to reference wire Type S thermocouples ranging from +1.4 percent to -3.6 percent, and standard deviation of eight samples of 2.07 percent.

The drift in thin film thermocouple indicated temperature with time during 1250 K gas flow cycling tests of eight samples was generally downward at a rate of less than 0.1 percent per hour.

Following these tests, a further study was made of the platinum adherence problem and related experiments were performed. As a result, the following techniques are considered worthy of further investigation:

1. Field-assisted bonding
2. Reactive sputtering
3. Precoats or bond coats between the platinum and the alumina.

These techniques will be investigated in Phase II.

## 7.0 REFERENCES

1. Burger, H. C., and VanCitter, P. H., "Preparation of Bismuth-Antimony Vacuum Thermal Elements by Vaporization", Z. Phys., V. 66, 1930, p. 210.
2. Harris, L. and Johnson, E. A., "Technique for Sputtering Sensitive Thermocouples", Rev. Sci. Inst., 5, 1934, p. 153.
3. Benderskey, D., "A Special Thermocouple for Measuring Transient Temperatures", Mech. Engr., 1953, 75, 117.
4. Dils, R. R. and Follansbee, P. S., "High Temperature Sputtered Surface Sensors", ISA, April 1975 meeting.
5. Dils, R. R. and Follansbee, P. S., "Superalloy Sensors", presentation at the Third International Symposium on Superalloys, Seven Springs, PA, Sept. 1 76.
6. Lieber, C. H., Mazaris, G. A., and Brandhorst, H. W., "Turbine Blade Metal Temperature Measurement with a Sputtered Thin Film Chromel-Alumel Thermocouple", NASA TM-X-71844.
7. Giggins, C. S. and Pettit, F. S., "Oxide Scale Adherence Mechanisms", Report No. PWA-5042, USAF/PWA Contract F33615-72-C-1702.
8. Sylvester, R. T. and Albright, C. E., "Thermal Compression Bonding of Copper", Sandia Laboratories Report SLA-73-0568, July 1973.
9. Smeggil, J. G., "The Effect of NaCl(g) on the Oxidation of NiAl", J. Electrochem Soc. Sol. State Sci. and Tech., Aug. 1978.
10. Milek, J. T., "Aluminum Oxide Data Sheets", DSA AD 434173.
11. D. M. Mattox, "Influence of Oxygen on the Adherence of Gold Films to Oxide Substrates", J. App. Phys., v. 37, n. 9, Aug. 1966.
12. Pomerantz, D. I., "Methods to Improve the Adherence of Metal Films Deposited on Glass Substrates", U. S. Patent 3,904,782, 1973 (Mallory).
13. Revitz, M., et al, "Method of Adhering Gold to an Insulating Layer on a Semiconductor Substrate", U. S. Patent 3,717,563 (1969) (IBM).
14. Bryant, W. A., and Meier, G. H., "Factors Affecting the Adherence of CVD Coatings", J. Vac. Sci. Tech., v. 11, n. 4, 1974.
15. Coleman, W. J., "Adherence Testing of Biased Sputtered Films for Isotope Encapsulation," 14th Annual Conference, Soc. of Vac. Coaters, Miami, March 1971.

16. Kortlandt, J., "Light Sensitive CdS Thin Films with Temperature Resistant Contacts", Microelectronics and Reliability, v 10, p 261-267, Pergamon Press, 1971.
17. Rand, M. J., "Chemical Vapor Deposition of Thin-Film Platinum," J. Electrochem Soc., v 120 n 5, 1973.
18. Fukutomi, M., et al, "Molybdenum Coating of Vanadium by CVD," J. of the Less Common Metals, 48 (1976) 65-77 (Netherlands).
19. Katz, G., "Adhesion of Copper Films to Aluminum Oxide Using A spinel Structure Interface," Thin Solid Films, 33 (1976) 99-105.
20. Sharpe, W. N. and Martin, D. R., "An Optical Gage for Strain/Displacement Measurement at High Temperature Near Fatigue Crack Tips", AFML-TR-77-153.
21. Hirsch, E. H., and Varga, I. K., "The Effect of Ion Irradiation on the Adherence of Germanium Films," Thin Solid Films, 52 (1978) 445-452.
22. Poate, J. M., Tu, K. N., and Mayer, J. W., Thin Films - Interdiffusion and Reactions, John Wiley & Sons, 1978.
23. Bube, K. R., and Hitch, T. T., "Basic Adherence Mechanisms in Thick and Thin Films," PRRL-78-Cr-5, 1978 (and authors' previous contract reports under same title).
24. Masterton, W. L. and Slowinski, E. J., Chemical Principles, W. B. Saunders Co., 1973.
25. Hecq, M. and Hecq, A., Notes on Platinum Monoxide, J. Less Common Metals, 1977, 56 (1), 133-136
26. Bay, N., "Cold Pressure Welding", ASME J. of Eng'g for Industry, v. 101, May 1979.